Bioorganic Chemistry 145 (2024) 107233

Contents lists available at ScienceDirect

Bioorganic Chemistry

journal homepage: www.elsevier.com/locate/bioorg

Targeting dihydroceramide desaturase 1 (Des1): Syntheses of ceramide analogues with a rigid scaffold, inhibitory assays, and AlphaFold2-assisted structural insights reveal cyclopropenone PR280 as a potent inhibitor☆

Pablo Rivero [a], Varbina Ivanova [b], Xavier Barril [b], Mireia Casampere [c], Josefina Casas [c], Gemma Fabriàs [c], Yolanda Díaz [a,*], M. Isabel Matheu [a,*]

[a] Universitat Rovira i Virgili, Departament de Química Analítica i Química Orgànica, Faculty of Chemistry, C/Marcel.lí Domingo 1, Tarragona 43007, Spain
[b] Universitat de Barcelona, Department of Physical Chemistry, Faculty of Pharmacy, Av. Joan XXIII s/n, Barcelona 08028, Spain
[c] Institute for Advanced Chemistry of Catalonia (IQAC-CSIC), Department of Biological Chemistry, C/Jordi Girona 18-26, Barcelona 08034, Spain

ARTICLE INFO

Keywords:
PR280
Dihydroceramide desaturase 1
AlphaFold2
Ceramide derivatives
Des1 inhibition
Organic synthesis

ABSTRACT

Dihydroceramide desaturase 1 (Des1) catalyzes the formation of a C—C double bond in dihydroceramide to furnish ceramide. Inhibition of Des1 is related to cell cycle arrest and programmed cell death. The lack of the Des1 crystalline structure, as well as that of a close homologue, hampers the detailed understanding of its inhibition mechanism and difficults the design of new inhibitors, thus making Des1 a strategic target. Based on previous structure-activity studies, different ceramides containing rigid scaffolds were designed. The synthesis and evaluation of these compounds as Des1 inhibitors allowed the identification of **PR280** as a better Des 1 inhibitor *in vitro* (IC_{50} = 700 nM) than **GT11** and **XM462**, the current reference inhibitors. This cyclopropenone ceramide was obtained in a 6-step synthesis with a 24 % overall yield. The highly confident 3D structure of Des1, recently predicted by AlphaFold2, served as the basis for conducting docking studies of known Des1 inhibitors and the ceramide derivatives synthesized by us in this study. For this purpose, a complete holoprotein structure was previously constructed. This study has allowed a better knowledge of key ligand-enzyme interactions for Des1 inhibitory activity. Furthermore, it sheds some light on the inhibition mechanism of **GT11**.

1. Introduction

Dihydroceramide desaturase 1 (Des1), is a membrane protein that catalyzes the formation of the *E*-configured double bond in C4-C5 positions in dihydroceramide (dhCer) to furnish ceramide (Cer) in the *de novo* synthesis pathway of this sphingolipid (Scheme 1) [1].

Regarding the active site, Des1 contains a non-heme dioxo-diiron species as a prosthetic group that specifically abstracts the C4 hydrogen atom from dihydroceramide *via* a rate-limiting step to form a very short-lived radical intermediate, followed by the fast elimination of a hydrogen at C5 to give ceramide [2].

Inhibition of Des1 would cause an accumulation of dhCer, a sphingolipid regarded as biologically inactive for a long time. However, studies in the last decade demonstrate the implication of dhCer in various biological processes [2,3], dhCer accumulation being related to autophagy induction and cell cycle arrest in cancer cells [4].

The scarce number of Des1 inhibitors described to date and the lack of a crystalline structure of the enzyme hamper the detailed understanding of its inhibition mechanism. Moreover, unlike other membrane proteins, (e.g. the G-protein coupled receptors), no close homologue existed for Des1 in the protein data bank (PDB), which made homology modelling impossible for this protein. Overall, there was no reasonable Des1 model available before the development of AlphaFold2, and therefore, Des1 represents a strategic target (Scheme 1).

Among the scarce pool of Des1 inhibitors documented so far, **GT11** was the first to be repored [5]. This C8-*N*-acylated-cyclopropenyl ceramide (Scheme 2a) induces Des1 inhibition in rat liver microsomes with a IC_{50} = 20 μM at substrate concentration of 50 μM, being also active in primary cultured cerebellar neurons [6].

Different *N*-acylated derivatives of this ceramide were described. However, only the *N*-hexanoyl and *N*-decanoyl **GT11** analogues (Scheme 2a) retained inhibitory activity (IC_{50} values of 31 and 13 μM

☆ Dedicated to Professor Sergio Castillón.

* Corresponding authors.
E-mail addresses: yolanda.diaz@urv.cat (Y. Díaz), maribel.matheu@urv.cat (M.I. Matheu).

https://doi.org/10.1016/j.bioorg.2024.107233
Received 9 October 2023; Received in revised form 4 January 2024; Accepted 19 February 2024
Available online 23 February 2024
0045-2068/© 2024 The Author(s). Published by Elsevier Inc. This is an open access article under the CC BY-NC-ND license (http://creativecommons.org/licenses/by-nc-nd/4.0/).

respectively) [7]. Inhibition by reaction of the cyclopropene ring with a cysteine residue in the active site of the enzyme has been suggested [5]. Nevertheless, this aspect has not been confirmed yet.

XM462 (Scheme 2a), with a -CH_2S- moiety replacing the natural C4-C5 ethylene scaffold, stands out among the few other ceramide Des1 inhibitors described [8]. The incorporation of a sulphur atom into the sphingoid base on this compound is justified on the activity of some thio fatty acids as fatty acyl-CoA desaturase inhibitors [9].

Structure-activity relationship (SAR) studies of **GT11** analogs [10], **XM462** derivatives [11] and a few other sphingolipid-based inhibitors [12] enabled the identification of critical structural features for the inhibition of Des1 activity by ceramide-type compounds (Scheme 2b). These requirements include: a) a (2*S*,3*R*)-configured aminoalcohol moiety, b) the presence of free hydroxyl groups at positions C-1 and C-3, and c) a secondary amide functionality. In addition, the presence of short *N*- acyloyl chains has been related to a good degree of cell permeability [7].

In our pursuit of a more potent ceramide-type Des1 inhibitor, guided by the aforementioned principles, we considered the possibility of integrating an alternative rigid cyclic framework at C4-C5 positions, related to that found in **GT11**. This structural variation could potentially enhance interactions within the enzyme's active site. Considering our experience in the synthesis of sphingolipids [13], we envisioned the design of *N*-acyl sphingoid bases as potential Des1 inhibitors containing 1,4- or 1,5-disubstituted 1,2,3-triazoles (Scheme 2c, **1–2**, respectively); a 2,4-disubstituted furan system (Scheme 2c, **3**) [14] as well as a cyclopropenone moiety (Scheme 2c, **4**) as rigid spacers between the headgroup and the lipophilic tail. Additionally, short *N*-hexanoyl (**a**), octanoyl (**b**) and decanoyl (**c**) derivatives were proposed to generate diversity and facilitate cell permeability. The design of the complementary 1,4- and 1,5- regioisomeric disubstituted 1,2,3-triazole systems arises from the knowledge that double bond geometry matters in Des1 inhibition [15].

Besides aiming at an effective ceramide-type inhibitor for Des1, this work also intends to solve some uncertainties related to the inhibition of this enzyme, since structure-activity studies conducted so far have not been able to provide with an answer (Scheme 2). In this regard, other objectives of the work are: a) to provide evidence allowing to confirm or rule out the proposed inhibition mechanism of **GT11** through reaction of the cyclopropene moiety with a cysteine residue in Des1; b) to have a better knowledge of key ligand-enzyme interactions for Des1 inhibitory activity; c) to explore the effects of having a rigid cyclic framework other than cyclopropene in the inhibitory activity of ceramide analogs.

To address these questions, we implemented the syntheses of the aforementioned analogs with the construction of a complete holoprotein model of Des1 based on the structure of the enzyme predicted by AlphaFold2. Docking studies of known Des1 inhibitors as well as the ceramide analogues synthesized in our laboratory were subsequently performed with the constructed dioxo diiron-Des1 system.

2. Results and discussion

2.1. Synthesis of ceramide analogues and Des1 inhibitory activity evaluation

Analogues having 1,4- and 1,5-disubstituted 1,2,3-triazole systems (**1a-c**, **2a-c**) were obtained by diastereoselective nucleophilic addition of lithium trimethylsilyl acetylide derivative to (*S*)-Garner's aldehyde. The described methodology towards **5** [16] was improved via *one-pot* ethynylation and catalytic desilylation [17] performing the addition reaction at −55 °C. This adapted procedure allowed obtaining intermediate **5**, as the only diastereoisomer, in 87 % yield from Garner's aldehyde (Scheme 3). Subsequent Cu(I) catalyzed azide-alkyne 1,3-dipolar cycloaddition (CuAAC) [18], gave efficient access (98 % yield) to 1,4-disubstituted triazole motif [19] in compound **6**. Deprotection of both the isopropylidene and the Boc groups in a single step by using a mixture of TFA/H_2O, resulted in the formation of aminodiol **7**. Final *N*-acylation of **7** with hexanoic, octanoic and decanoic acid using EDC in the presence of HOBt, furnished ceramide analogues **1a-c** in a 4-step syntheses with overall yields of 28 %, 31 % and 29 % respectively (Scheme 3).

Additionally, the 1,5-disubstituted-1,2,3-triazole series of ceramides **2a-c**, were accessed from **5** through a less conventional alkyne-azide cycloaddition. The reaction was assayed with Cp_2Ni/Xantphos [20], Cp*RhCl$(PPh_3)_2$ [21], and Cp*RuCl(COD) [22] as catalytic systems under different conditions (Table S1, Supporting Information). The use of Cp*RuCl(COD) in toluene at room temperature provided the best result, yielding compound **8** in 72 % yield with no traces of the 1,4-regioisomer [23]. After hydrolysis of compound **9** and *N*-acylation, ceramide derivatives **2a-c** were obtained in four steps from Garner's aldehyde in 29–33 % total yield (Scheme 3). X-ray crystallography of compound **2c** confirmed the desired *anti*-relative configuration of the 2-amido-3-hydroxy moiety (see Supporting information).

Moreover, 2,5-disubtituted furan compounds (**3a-c**) were synthesized by sequential furan alkylation using 2-furyllithium as nucleophile to obtain 2-dodecylfuran **10** [24] in a 99 % yield. Subsequent diastereoselective addition of (5-alkyl-2-furyl)lithium to (*S*)-Garner's aldehyde, afforded alcohol **11** in a 7:1 *anti/syn* ratio.

Next deprotection step was not obvious. Treatment of compound **11** with either TFA/H_2O, HCl 2 M in Et_2O, TMSBr in CH_2Cl_2 or acetyl chloride in anhydrous MeOH [25] led to product decomposition (probably via furan opening or Piancatelli rearrangement of the

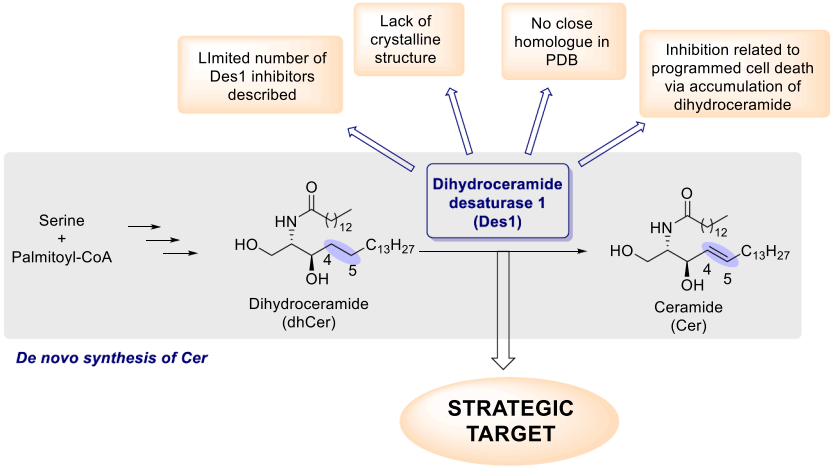

Scheme 1. Dihydroceramide desaturase 1 (Des1), a strategic target.

furfurylcarbinol moiety) [26], or 3-*O*-methyl derivatives (most likely via carbocation formation and subsequent methanol trapping) when this solvent was used. Previous protection of OH-3 as acetyl ester or *tert*-butyldiphenylsilyl ether was not effective either. Eventually, treatment of **11** with TMSOTf/Et_3N and TBAF led to aminodiol **12** in 97 % yield. Final *N*-acylation afforded furan derivatives **3a-c** in 48–61 % overall yield (Scheme 4).

Des1 inhibition activity of **1a-c**, **2a-c** and **3a-c** was tested *in vitro* with intact T98 tumor cells using **XM462** or **GT11** as positive controls of inhibition in the presence of fluorescent dhCerC6NBD (*N*-[6-[(7nitro2-1,3-benzoxadiazol-4-yl)amino]hexanoyl]- D -*erythro*-sphinganine) as substrate.

Triazole derivatives (**1a-c**, **2a-c**) caused statistically significant Des1 inhibition in intact T98 cells ranging from 10 % to 50 %, at 10 μM concentration, the 1,4-disubstituted triazole *N*-decanoyl chain ceramide analog **2c** reaching the maximum inhibition. As for the furan series, only the *N*-hexanoyl chain ceramide **3a** showed a significant 40 % of inhibitory activity in intact cells (Fig. 1).

Additionally, Des1 inhibition experiments using **1a-c**, **2a-c** and **3a-c** in T98 cell lysates resulted negative (Fig. 1). Since none of these derivatives inhibits Des1 in T98 cell lysates, the moderate inhibition observed in intact cells might be considered indirect, probably not affecting therefore the enzyme active site but the previous electron transport chain instead or via a down-regulation of Des1 gene expression.

Thus, the absence of Des1 inhibition in lysates displayed by compounds **1a-c**, **2a-c**, and **3a-c** suggests a limited interaction of these ligands within the enzyme's active site. Hypothesizing that lack of direct inhibitory activity could arise from the large size of the ring in these compounds, we focused our attention on the installation of a smaller ring as a rigid scaffold.

In this regard, we envisioned the installation of a cyclopropenone moiety as a linker for achieving inhibition. First, it retains the small steric volume and the *cis*-configuration than that of cyclopropene moiety. Besides, the oxo moiety in this functionality could well be engaged in favourable interactions with the iron center in the prosthetic group. The selection of a cyclopropenone as an alternative functionality to cyclopropene is not as straightforward as it might seem, taking into account that cyclopropenone fatty acids proved inactive as inhibitors of fatty acyl desaturases [27]. Furthermore, if the proposed Des1 inhibition caused by **GT11** arises, as described, from reaction with a cysteine residue within the active site of Des1, a comparable response from a cyclopropenone functionality is not readily apparent [27,28].

The synthesis of cyclopropenone derivative, named **PR280**, was carried out as depicted in Scheme 5. The first step involved a [2+1] cycloaddition of pentadec-1-yne with trifluoromethyltrimethylsilane (Ruppert–Prakash reagent) as a difluorocarbene source [29]. The difluorocyclopropene product **13** generated could not be isolated due to its fast hydrolysis, but fortunately, the reaction crude was clean enough to confirm the formation of the desired compound by ^{19}F NMR analysis

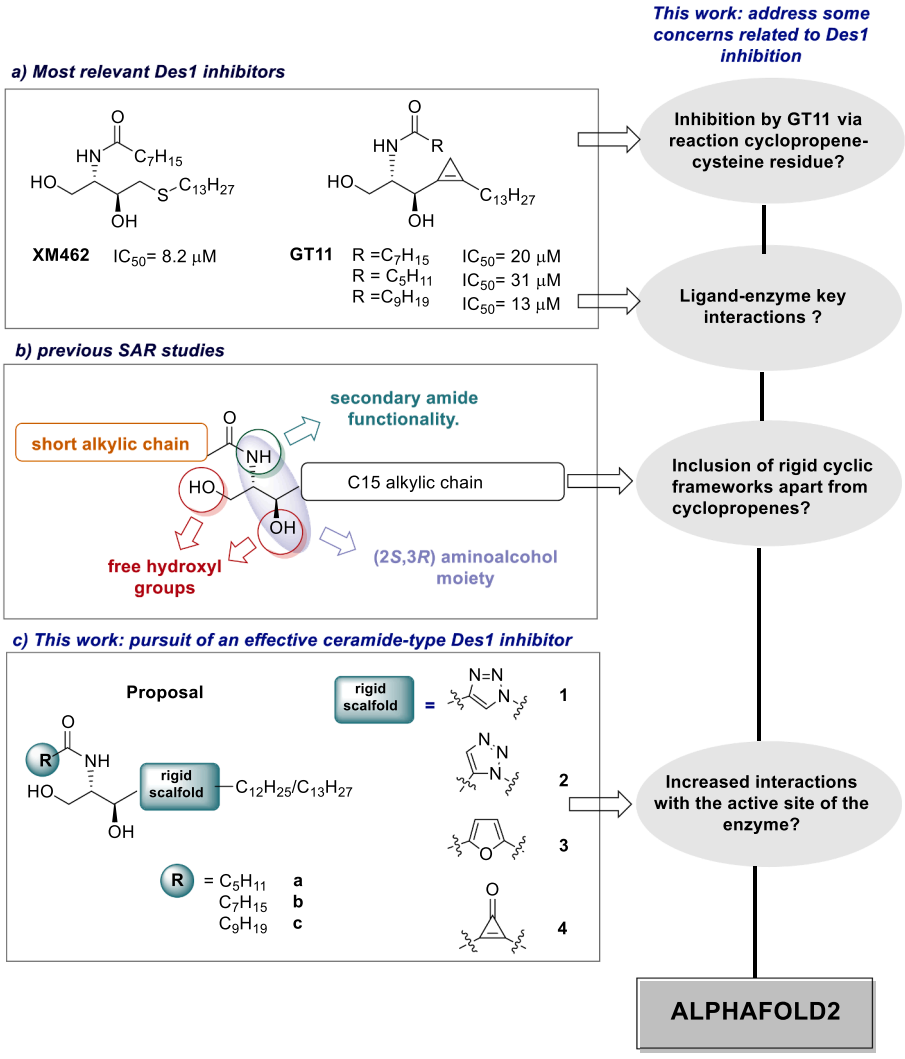

Scheme 2. Antecedents and aims of the work.

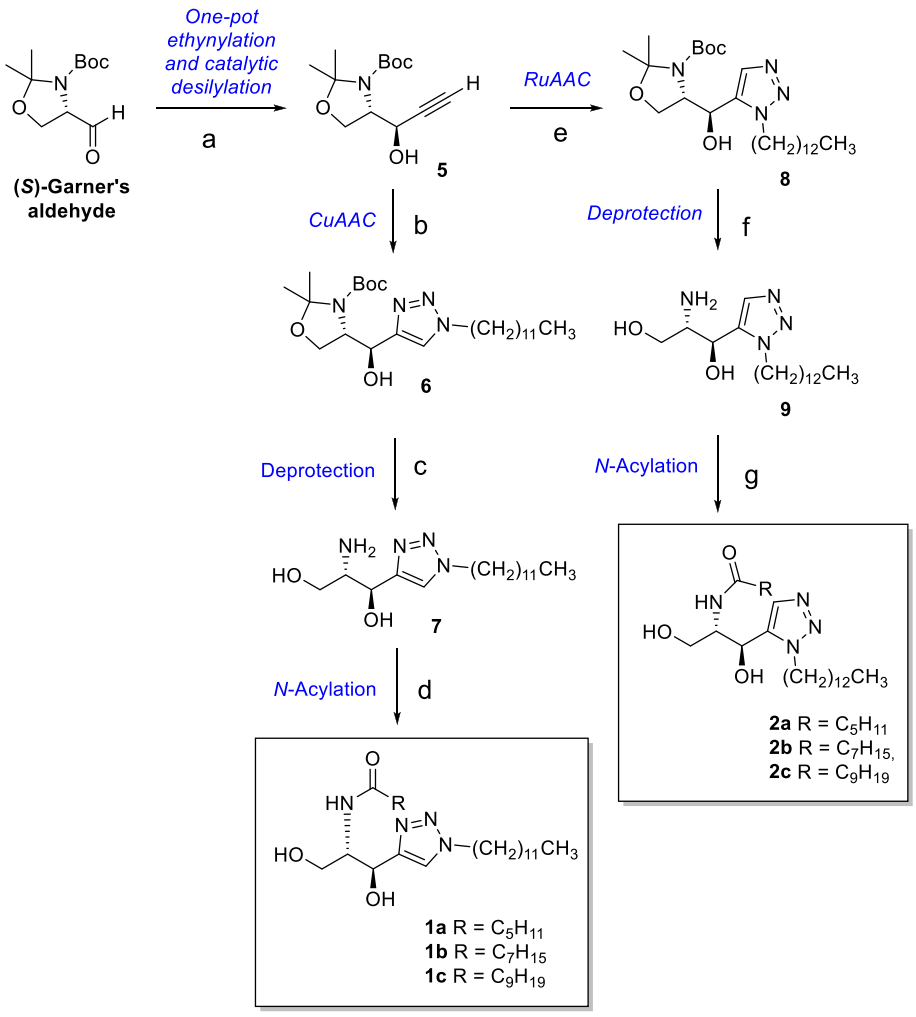

Scheme 3. Syntheses of 1,4- and 1,5-disubstituted-1,2,3-triazole ceramide analogs (**1a-c**, **2a-c**). Reagents and conditions: (a) 1. trimethylsilylacetylide, BuLi, HMPA/THF, −55 °C. 2. TBAF (0.1 eq.)/THF, r.t., 87 %. (b) $N_3(CH_2)_{11}CH_3$, $CuSO_4{\cdot}H_2O$ (5.5 % mol), sodium ascorbate, H_2O/CH_2Cl_2, r.t., 98 %. (c) TFA/H_2O (10:1), r.t. 54 %. (d) RCOOH, EDC·HCl, HOBt, CH_2Cl_2, r.t. 62 % (**1a**, from hexanoic acid), 67 % (**1b**, from octanoic acid), 63 % (**1c**, from decanoic acid). (e) $N_3(CH_2)_{12}CH_3$, Cp*RuCl (COD) (5 mol %), Toluene, r.t., 72 %. (f) TFA/H_2O (10:1), r.t., 73 %. (g) RCOOH, EDC·HCl, HOBt, CH_2Cl_2, 64 % (**2a**, from hexanoic acid), 70 % (**2b**, from octanoic acid), 72 % (**2c**, from decanoic acid).

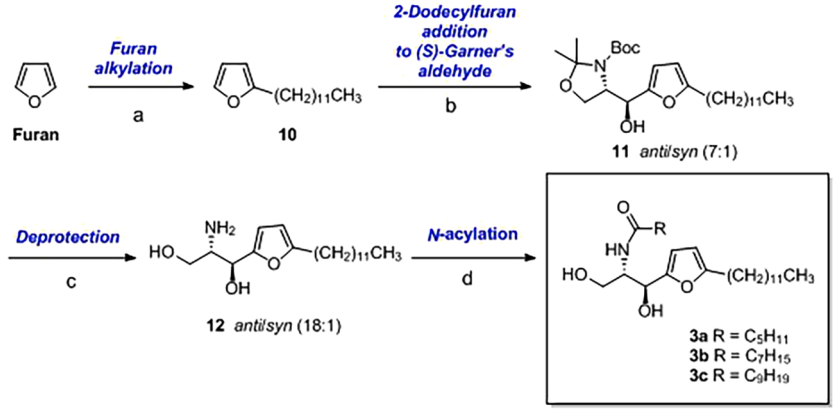

Scheme 4. Syntheses of 2,5-disubstituted furan ceramide analogs (**3a-c**). Reagents and conditions: (a) 1. BuLi, THF, 0 °C. 2. $CH_3(CH_2)_{11}Br$, THF, r.t., 99 %. (b) 1. BuLi, HMPA, THF, 0 °C. 2. (*S*)-Garner's aldehyde, THF, −55 °C, 83 %. (c) 1. TMSOTf, Et_3N, CH_2Cl_2, 0 °C. 2. TBAF (1 M), THF, r.t., 97 %. (d) RCOOH, HOBt, EDC, CH_2Cl_2, r.t., 77 % (**3a**, from hexanoic acid), 60 % (**3b**, from octanoic acid), 73 % (**3c**, from deecanoic acid).

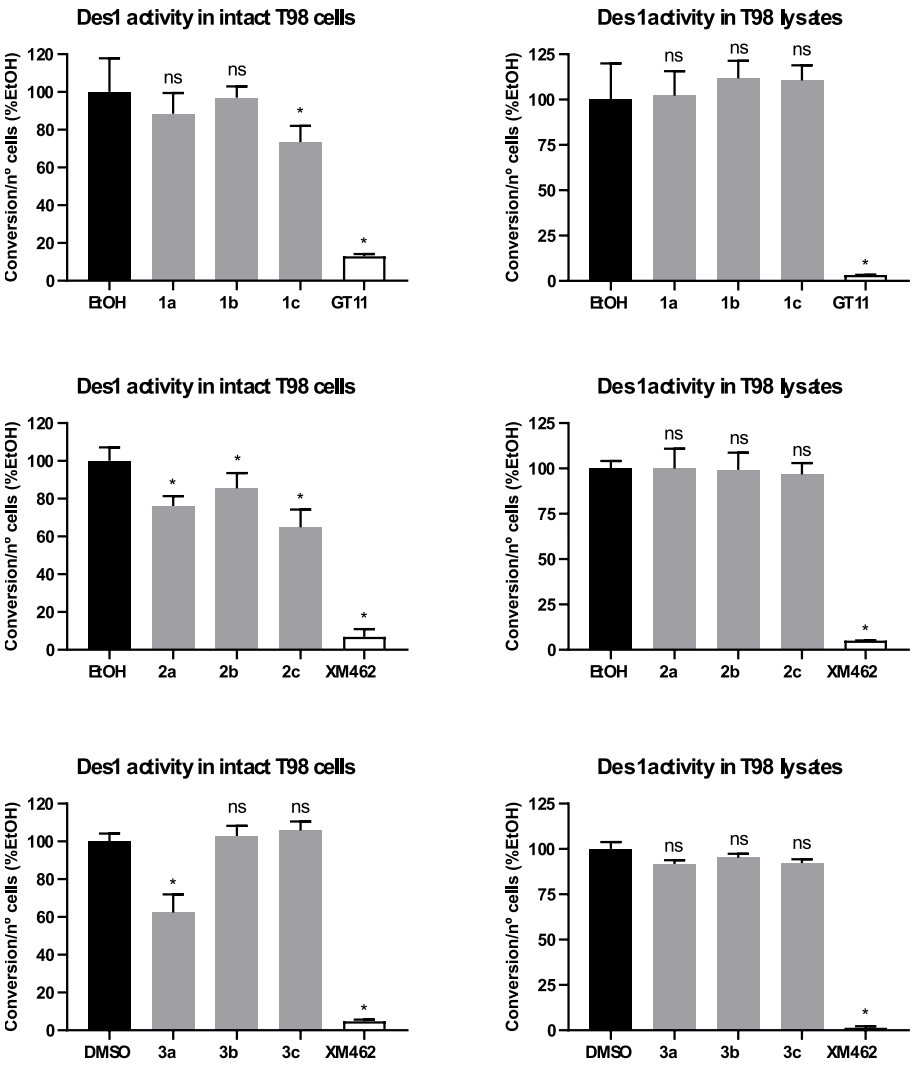

Fig. 1. Effect of compounds **1a-c**, **2a-c**, **3a-c** on the activity of Des1. T98G cell lysates or T98G cells were incubated with EtOH (control), compounds **1a-c**, **2a-c**, **3a-c** (10 μM) or **GT11**/**XM462** (10 μM) (positive control). The Des1 substrate (dhCerC6NBD, 10 μM) was then added and cells were collected 4 h later. Medium and cell samples were analyzed by HPLC coupled to a fluorescence detector. Values are the mean of 2 independent experiments with triplicates. Asterisks indicate statistical significant over DMSO or EtOH controls at $P < 0.05$ (unpaired, two-tailed, *t*—test).

(see Supporting Information).

Reaction of crude **13** with silica gel in a mixture of Hexane/AcOH then produced cyclopropenone **14** in almost quantitative yield. The cyclopropenone formation can be rationalized by the initial release of a fluoride ion that would result in the formation of the aromatic fluorocyclopropenyl cation, which could react with water, leading to the cyclopropenone derivative after HF elimination [30].

The carbonyl group of compound **14** was then protected to prevent side reactions under the strong basic conditions used in the next step. The reaction was conducted using neopentylglycol in the presence of triethyloxonium tetrafluoroborate to furnish **15** in 89 % yield. Subsequent diastereoselective addition of the lithium ylide obtained from the protected derivative **15** to (*S*)-Garner's aldehyde [31] under Felkin-Anh control furnished alcohol **16** (76 % yield) as a single diastereomer (mixture of rotamers, see Supporting information), with the desired *anti*-aminoalcohol stereochemistry.

Full deprotection of product **16** using HCl in ethereal solution led to compound **17** as the corresponding chloride salt, from which free aminoalcohol **17** was obtained (62 % yield) after purification by flash column chromatography with neutralized silica gel. With aminodiol **17** in hand, final *N*-acylation with octanoic acid afforded compound **PR280** in 60 % yield. As ceramide analogues **1a-c**, **2a-c** and **3a-c** had shown similar inhibition results in cell lysates regardless the length of the *N*-acyl chain, only the *N*-octanoyl chain (also present in **GT11**) was introduced. Altogether, the target ceramide analogue was obtained in a 6-step synthesis in an overall yield of 24 %.

The confirmation of the *anti*-relative configuration of the 2-amido-3-hydroxy moiety, crucial for inhibitory activity, was obtained via X-ray crystallography (Fig. 2, for details see Supporting information).

Inhibitory activity of **PR280** on Des1 using DhCerC6NBD as a substrate was evaluated (Fig. 3). Thus, **PR280** displayed an 86 % of inhibition (at 10 μM) in intact T98-cells, a similar value to that of **XM462** (85 % at 10 μM). More importantly, this compound showed a remarkable 92 % of inhibition in T98 cell lysates, surpassing the value obtained for **XM462** (78 %) which suggests an improved direct inhibition effect against Des1.

The Des1 inhibition induced by **PR280** is dose-dependent with an IC_{50} value of 700 nM (10 μM dhCerC6NBD substrate, Fig. 4), lower than that reported for **GT11** (20 μM) [5] and **XM462** (8.2 μM) [8], respectively.

To discard a Des1 inhibition by reaction of the cyclopropenone moiety of **PR280** with a cysteine residue of Des1, **PR280** was subjected to react with ethanethiol under the same conditions assayed by J. Quintana *et al.* [27] **PR280** proved to be unreactive after 6 days of

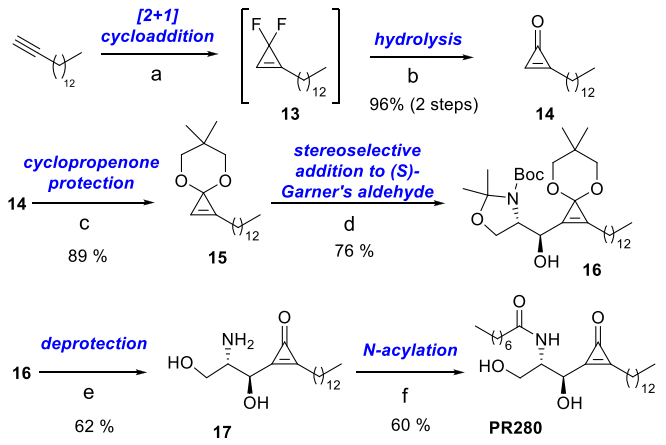

Scheme 5. Synthesis of **PR280**. Reagents and conditions: (a) NaI, $TMSCF_3$, dry THF, 110 °C, overnight. (b) Silica, Hexane/AcOH (aq. sol.) (99:1), r.t., overnight, 96 % (2 steps) (c) Neopentylglycol, $BF_4{\cdot}OEt_3$, dry CH_2Cl_2, dry Et_3N, r.t., 89 %. (d) 1. BuLi, HMPA, dry THF, −55 °C, 30 min. 2. (*S*)-Garner's aldehyde, dry THF, −55 °C, overnight, 76 %. (e) HCl (2 M in Et_2O), H_2O, r.t., 2 h. purification in CH_2Cl_2/MeOH/NH_4OH (9:1:0.1), r.t., 62 % (f) HOBt, EDC, octanoic acid, dry CH_2Cl_2, r.t. overnight, 60 %.

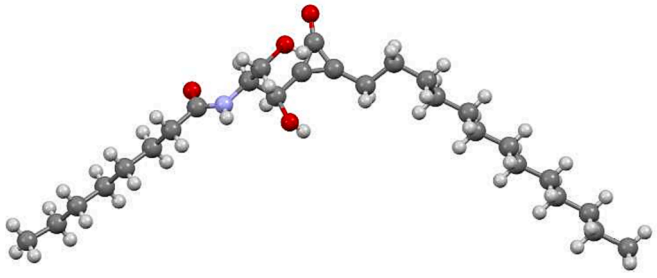

Fig. 2. X-ray analysis of **PR280** [CDCC: 2252495] confirming the desired *anti* relative configuration of the 2-amido-3-alcohol moiety.

reaction, as confirmed by ^{1}H NMR (Fig. S52, Supporting Information).

Thus, the synthesized triazole and furan-derived compounds showed moderate indirect enzyme inhibition in intact cells and no direct inhibition in lysates. However, the cyclopropenone derivative **PR280** displays a strong direct inhibition of Des1. This suggests that while the former are not capable of interacting strongly with the enzyme's active site, the latter does. Nevertheless, this outcome presents a challenge for straightforward interpretation, as all compounds meet the structural requirements for Des1 inhibition outlined in the current state of SAR studies.

2.2. Docking study

With the experimental process in course, AlphaFold2 appeared as a powerful tool for the 3D prediction of proteins [32]. The use of this software is specially interesting for targets like Des1, where the experimentally-determined 3D structure of the enzyme from the PDB archive or that of a close homologue is lacking, making the prediction of crucial protein-ligand interactions exceptionally challenging.

To our delight, the model of Des1 predicted by Alpha Fold2 (AF-O15121-F1-model_v4) has a very high confidence level (Fig. 5, A and B), with a per-residue estimate of its confidence (pLDDT) greater than 90 on a scale from 0 to 100. It is important to note that this situation is not very common: the proportion of proteins unavailable by homology studies showing high confidence by Alphafold2 is rather low (~15 %) [33].

With this perspective, we set out to construct a 3D model of Des1 based on the AlphaFold2 predictions. Since the AlphaFold2 does not provide information on the location of prosthetic groups [34], the most plausible location for the Fe_2O_2 species was estimated based on the presence of donor amino acid residues. In this regard, AlphaFold2 model of Des1 showed an area of high concentration of histidines at the end of well-defined deep binding pocket of the enzyme, mostly surrounded by a highly hydrophobic environment.

Thus, the Fe_2O_2 system was positioned in this area so that one iron atom could coordinate to five histidine residues (His89, His93, His128,

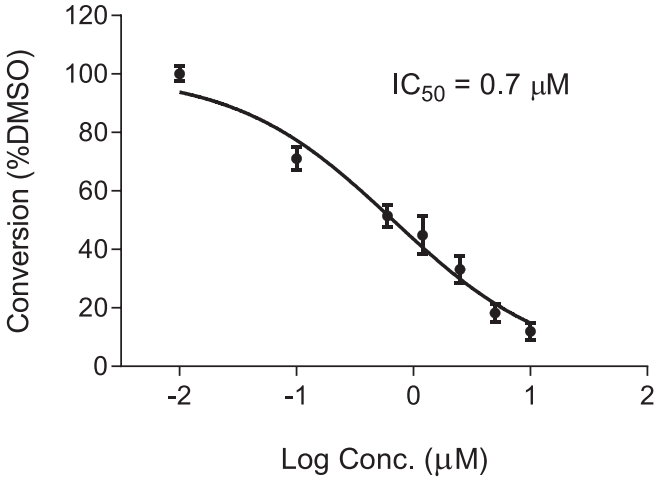

Fig. 4. Concentration-dependence of dihydroceramide desaturase inhibition by **PR280** in T98 lysates. Enzyme activity was determined as indicated in the experimental section using a substrate concentration of 10 μM and different concentrations of **PR280** (0.1, 0.6, 1.2, 2.5, 5, and 10 μM). Data correspond to the mean ± SD of 2 independent experiments with three replicates. The calculated IC_{50} value is 700 nM.

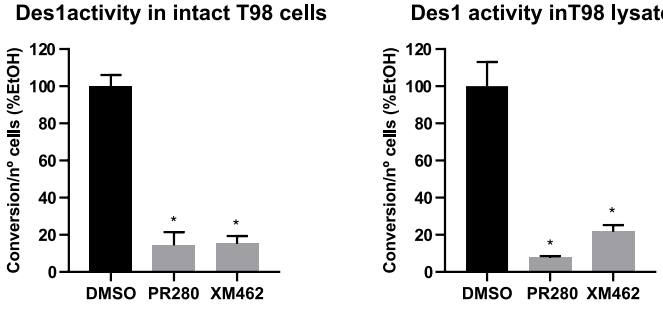

Fig. 3. Effect of **PR280** on Des1 activity. T98G cell lysates or T98G cells were incubated with ethanol (control), **PR280** (10 μM) or **XM462** (10 μM) (positive control). Then, the Des1 substrate (dhCerC6NBD, 10 μM) was added and cells were collected 4 h later. Medium and cell samples were analyzed by HPLC coupled to a fluorescence detector. Values are the mean of 2 independent experiments with triplicates. Asterisks indicate statistical significance over vehicle (EtOH) at $P < 0.0001$ (unpaired, two-tailed *t* test).

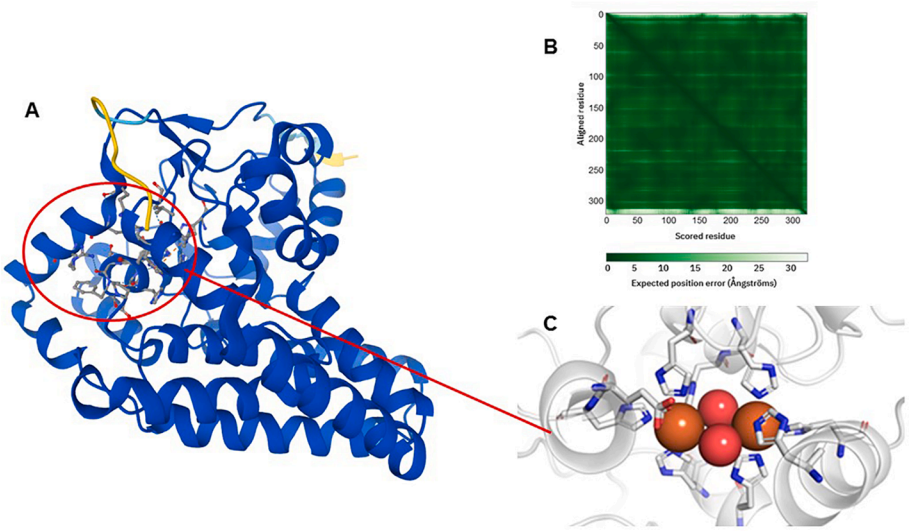

Fig. 5. A: AlphaFold structure of human Des1 (AF-O15121-F1-model_v4). Dark blue color shows a pLDDT > 90. B: predicted aligned error. The colour at position (x, y) indicates AlphaFold's expected position error at residue x, when the predicted and true structures are aligned on residue y. C: Detail of the Des1 deep pocket showing the constructed Fe_2O_2-Des1 complex. (For interpretation of the references to color in this figure legend, the reader is referred to the web version of this article.)

His132 and His262), and the second one to four histidine residues (His131, His233, His263, and His259) and a glutamic acid residue (Glu232) (Fig. 5C). The Fe_2O_2-Des1 complex was then prepared for docking studies with MOE software, using the protein preparation protocol [35].

A preliminary study of the constructed Fe_2O_2-Des1 model showed that there are no cysteine residues in the Des1 active site or nearby [36]. This piece of evidence could rule out the Des1 inhibition mechanism of **GT11** initially proposed arising from reaction of the cyclopropene moiety with a cysteine residue in the active site of the enzyme [5,37].

To gain insight into the key ligand-enzyme interactions that govern Des1 inhibition, docking studies of reference Des1 inhibitors (**GT11**, **XM462**) and the natural substrate dhCer were performed using the AlphaFold2-based Fe_2O_2-Des1 system model (Fig. 6).

The proposed binding mode for **GT11** showed a folded conformation of the hydrophobic chains of the sphingolipid (Fig. 6A) so that the methylene group in the cyclopropene ring was in close proximity to one of the iron metal centers [38]. Further analyzing this arrangement in the binding pocket, the OH-3 group of **GT11** hydrogen bonded to an oxygen at the dioxo-diiron complex, while the OH-1 participated in a hydrogen

Table 1
Summary of enzyme-ligand interactions identified.

Compound[a]	Tyr170	Tyr120	Glu232	Oxygen (Fe_2O_2)	Fe_2O_2 cluster proximity
GT11	OH-1 H-bond donor			OH-3 H-bond donor	Cyclic methylene group
XM462		OH-1 H-bond donor		OH-3 H-bond donor	S atom
DhCer	OH-1 H-bond donor				CH-4
PR280			OH-1 H-bond donor	OH-3 H-bond donor	Cyclopropenone oxo moiety

[a] A folded conformation of alkylic chains was observed in all cases.

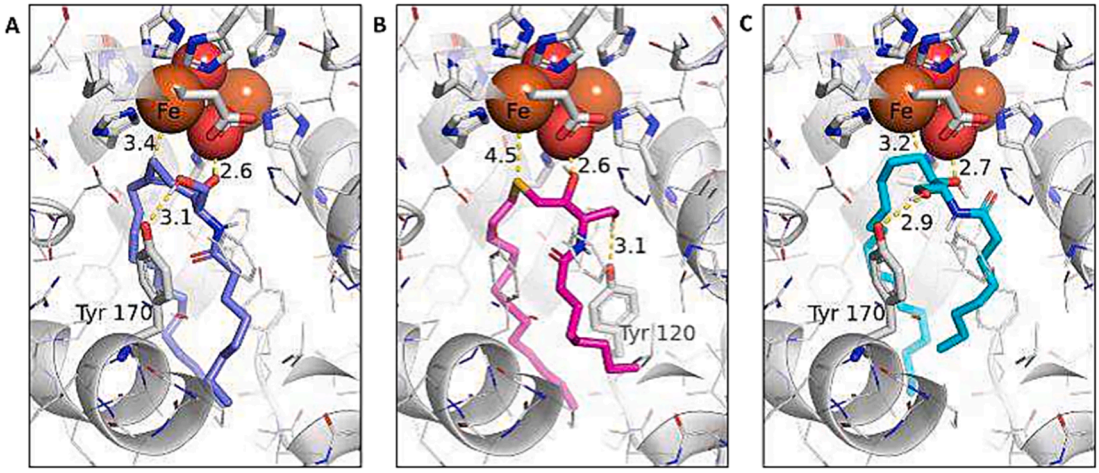

Fig. 6. Binding mode of **GT11** (A), **XM462** (B) and **dhCer** (C). Aminoacid residues involved in ligand-enzyme interactions are marked and indicated in sticks; those not involved in specific interactions are represented with lines. The length of interactions in Å is specified.

bond donor with Tyr170 (Table 1).

For compound **XM462,** a folded conformation was also observed (Fig. 6B). The best docking pose showed the same H-bond interaction between the oxygen atom at the complex and OH-3, as observed in **GT11**, thus bringing the sulfur atom in close proximity to the same iron metal center. Additionally, the OH-1 group participates as a hydrogen bond donor in the interaction with the Tyr120 phenolic group (Fig. 6B and Table 1).

The different orientation of OH-1 in **GT11** and **XM46**2 could be forced by the size of sulphur atom in the latter. Should the primary alcohol in **XM462** take a similar orientation to that of **GT11**, it could hydrogen bond to the sulfur atom [39], thus losing favorable interactions with the enzyme.

Based on this docking study, the main requisites for a good Des1 inhibitory activity in a ceramide-like ligand are: a) a folded conformation of the ligand in the Des1 active site; b) a close proximity of positions 4 or 5 of the ceramide to the Fe_2O_2 cluster; c) a hydrogen bond interaction of OH-3 with one of the oxygen atoms of the dioxo-diiron system; and d) the involvement of the primary hydroxyl group in a hydrogen bond (donor) interaction with a residue of the enzyme.The essential OH-1 hydrogen bond donor interaction with the enzyme was also observed in the natural substrate, dhCer (OH1-Tyr170 in Fig. 6C and Table 1), as well as an intramolecular hydrogen bond between OH-3 group and the carbonyl oxygen of the dhCer. It is important to highlight that in all the ligands studied, the most probable position of the amido group, is far from residues with which it could be engaged in polar interactions.

Molecular docking was also performed with the synthesized compounds **1b**, **2b** and **3b**. As ceramide analogues **1a-c**, **2a-c**, **3a-c** showed no inhibition in cell lysates regardless the length of the *N*-acyl chain, the study was only conducted with ceramide analogues **b**, containing the same acyl chain as **GT11** and **XM462**, for comparative purposes. Regarding compound **1b**, with a 1,4-disubstituted triazole core, the bulky size of the ring moiety might affect the folding of the structure and, as a result, the arrangement of the hydroxyl groups, thus leading to a loss of all the favourable H-bond interactions previously identified (Fig. 7A).

In comparison, the 1,5-disubstituted triazole ring of compound **2b**, which behaves like a *cis*-olefino mimetic surrogate, was able to approach the iron metal center and allowed the structure to fold more adequately (Fig. 7B). Thus, the position of the ring allowed the formation of the hydrogen bond between the OH-3 and the dioxo-diiron oxygen. However, the key H-bond donor interaction involving OH-1 group was not formed, possibly due to the ring's size or even its nature. Nevertheless, the hydroxyl group was able to establish an intramolecular hydrogen bond with the OH-3. For compound **3b**, with a 2,4-disubstituted furan core, similar in size to the triazole group, both OH-1 and OH-3 were unable to participate in favourable interactions, again due to the different arrangement of the heterocycle in relation to that of the cyclopropane moiety in **GT11** (Fig. 7C). Thus, the lack of key ligand-enzyme interactions observed in **GT11** and **XM462**, in particular the one involving the primary hydroxyl group, could explain the inability of ceramide analogs **1**–**3** to inhibit Des1 in cell lysates.

Finally, ceramide **PR280** was docked in the dioxo-diiron-Des1 complex (Fig. 8). The most probable binding mode showed hydrogen bond interactions of OH-3 with the dioxo-diiron oxygen atom while the OH-1 group formed a hydrogen bond with Glu232. The location of the cyclopropenone moiety, in close proximity to the iron complex, might be due to coordination of the oxo moiety to the iron center, thus stabilizing the folded conformation. The identification of the three crucial interactions, as outlined earlier, responsible for Des1 inhibition (proximity to Fe_2O_2 cluster, H-bonding with OH-1 and OH-3) offers a plausible explanation for the **PR280** strong inhibitory activity.

The consistency of the results obtained by inhibitory assays with those obtained from docking studies may well validate the 3D construct of the enzyme provided by Alphafold2.

The docking studies here presented are a first reasonable hypothesis, but not definitive, and will be complemented in the future with molecular dynamic simulations [40]. On the other hand, ongoing efforts in our group are being held to undertake the study of a large library of cyclopropenone-based inhibitors covering diversity sites in order to gain insight into the inhibition mode of this enzyme, and to expand the structure-activity relationship of these **PR280** derivatives. Eventually, inhibition assays of those with better-predicted inhibition profile, complemented with molecular dynamic simulations will enable us to validate the constructed Alphafold2-based model.

3. Conclusions

A small set of ceramide analogs containing 1,4-triazole, 1,5-triazole and cyclopropenone ring systems as rigid spacers between the polar headgroup and the fatty tail, and featuring different *N*-acylated chains to provide diversity, were synthetized and biologically and computationally evaluated as Des1 inhibitors, and further compared with reference inhibitors **GT11** and **XM462**. This study shows that five-membered ring scaffolds are not good surrogates of the cyclopropene moiety in **GT11**, the bulkyness of the ring probably causing a distortion of the optimal

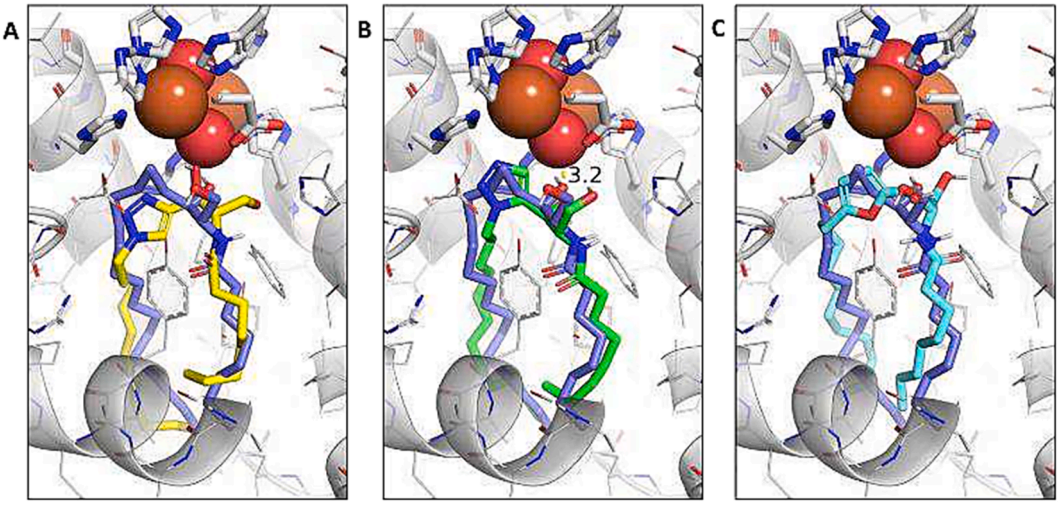

Fig. 7. Binding mode of **1b** (A, yellow), **2b** (B, yellow) and **3c** (C, grey) overlapped with that of **GT11** (blue). Interaction between OH-3 and the dioxo-diiron oxygen is indicated in the binding mode of product **2b** (B). (For interpretation of the references to color in this figure legend, the reader is referred to the web version of this article.)

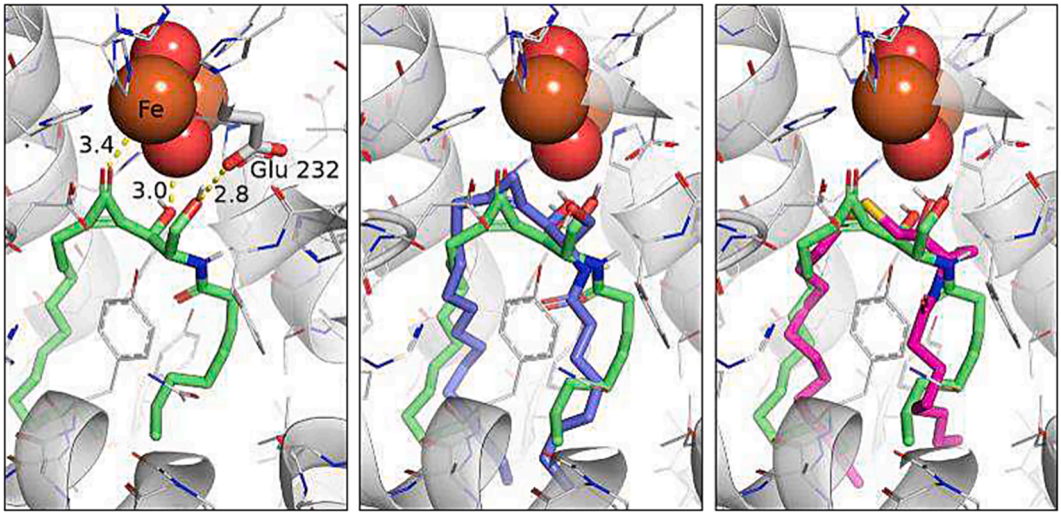

Fig. 8. Binding mode of **PR280** (A, green), overlapped with **GT11** (B, blue), and **XM462** (C, magenta). Amino acid residues involved in **PR280**-enzyme interactions are marked and indicated in sticks; those not involved in specific interactions are represented with lines (A). The length of interactions in Å is specified (A). (For interpretation of the references to color in this figure legend, the reader is referred to the web version of this article.)

position of the ligand in the active site of the enzyme. This piece of evidence could explain the lack of direct Des1 inhibitory activity displayed by these compounds.

Nevertheless, **PR280**, an *N*-octanoyl ceramide derivative with a cyclopropenone ring as a rigid scaffold, obtained in an efficient 6-step synthesis in 24 % overall yield, showed a very high *in vitro* Des 1 inhibitory activity in T98 lysates with IC_{50} value of 700 nM, being therefore more active than **XM462** and **GT11,** the current reference inhibitors [41].

To the best of our knowledge, this work provides the first reported example of the use of AlphaFold2 in the prediction of the 3D structure of Des1 to identify key ligand-protein interactions in well-known ceramide Des1 inhibitors, previous construction of the full Fe_2O_2-Des1 model. This information is relevant, due to the lack of the Des1 crystalline structure and the impossibility of conducting homology studies. The determinant interactions found were OH-1 and OH-3 hydrogen bonds with Des1 amino acid residues and Fe_2O_2 prosthetic group respectively, as well as a close location of atoms at positions 4 or 5 in the ceramide type ligand to the Fe_2O_2 cluster.

Docking experiments of the five-membered ring-analogues synthesized **1b**, **2b** and **3b** revealed the absence of key ligand-protein interactions necessary for inhibition, thus supporting the low Des1 inhibitory activity thereof.

Docking experiments of the cyclopropenone derivative **PR280** revealed the presence of the key ligand-protein interactions previously identified for inhibition, thus supporting its high *in vitro* Des1 inhibitory activity, in contrast with those of the corresponding inactive five-membered analogues.

As confirmed in this study, the active center of Des1 lacks any cysteine residue. This fact opens up the door to explore inhibition mechanisms for **GT11** different to those previously reported, involving a reaction of the cyclopropene moiety with a cysteine residue of the enzyme. The present study points out an alternative inhibition mechanism consisting of specific and strong non-covalent interactions of the ligand with polar residues and the prosthetic group located at the end of the long deep channel constituted by the active site. This perspective can also be applied to the inhibition offered by **PR280**. Thus, the present study may pave the way to gaining greater knowledge on Des1 inhibition.

4. Experimental section

4.1. General methods and synthetic procedures

All reactions sensitive to air and/or moisture were carried out in anhydrous conditions: performing vacuum-argon cycles in the flasks to be used, previously dried heating with a heating gun under vacuum, as well as transferring the reagents and solvents with cannulas or syringes previously purged with argon. The procedures described below are the ones that performed with the highest yield.

IR spectra were obtained with a JASCO FT/IR-680 plus infrared spectrophotometer with Fourier transform and visualized with the SpectraManager software (JASCO®). Optical rotations ($[\alpha]_D^{25}$) were obtained with Perkin-Elmer 241 polarimeter with a path length of 1.0 dm. Melting points (M.p.) were obtained with a Mettler Toledo DSC 822e. High–resolution mass spectra (HRMS) were recorded on an Agilent 1100 Series LC/MSD mass spectrometer with electrospray ionization (ESI). Exact *m/z* values are reported in Daltons. ^1H, ^{13}C, ^{19}F, COSY, HSQC and HMBC NMR spectra were obtained with a Varian Mercury VX 400 and visualized with the MestreNova software (MestreLab®).

The coupling constants (*J*) are described in Hz using the following abbreviations: s = singlet, d = doublet, t = triplet, q = quadruplet, p = quintuplet, m = multiplet, dd = doublet of doublets, dt = doublet of triplets, td = triplet of doublets, ap = apparent, br = broad. All spectra are referenced in relation to the residual signal of the deuterated solvent used.

Thin-layer chromatography was performed on 0.25 mm E. Merck® aluminum plates coated with 60 F_{254} silica, using p-anisaldehyde or $KMnO_4$ as developer as indicated. Chromatographic columns were performed by passing the mentioned solvent under pressure through Fluka® or Merck® silica gel 60 (230–400 mesh).

4.1.1. General procedure for N-acylation of aminodiol intermediates

Hexanoic acid (products **a**), octanoic acid (products **b**) or decanoic acid (products **c**) (0.14 mmol), EDC (0.14 mmol) and HOBt (0.14 mmol) were dissolved in dry CH_2Cl_2 (6.9 mL) and the solution was stirred at room temperature for 30 min. The resulting mixture was added over a solution of aminodiol **7**, **9**, **12** or **17** (0.092 mmol) in dry CH_2Cl_2 (7.5 mL) and stirred at r.t. overnight. After this time, water was added, both phases were separated, and the aqueous phase was extracted with CH_2Cl_2. The combined organic extracts were dried over anhydrous $MgSO_4$ and concentrated under vacuum to give a residue which was

purified by flash column chromatography on silica gel using CH_2Cl_2/MeOH mixtures.

4.1.2. (S)-tert-butyl 4-((R)-1-hydroxyprop-2-yn-1-yl)-2,2-dimethyloxazolidine-3-carboxylate (5)

Ethynyltrimethylsilane (0.25 mL, 1.77 mmol) was dissolved in dry THF (8.4 mL). The resulting solution was cooled down to −78 °C and BuLi solution (2.5 M in hexanes, 0.7 mL, 1.75 mmol) was added dropwise. The resulting mixture was stirred for 1 h at −78 °C. Then, HMPA (0.38 mL, 2.18 mmol) was added and the mixture was stirred for another additional hour. After this time, (S)-Garner's aldehyde (252 mg, 1.10 mmol) dissolved in dry THF (1 mL) was added. The mixture was warmed up to −55 °C and stirred at this temperature overnight (18 h.). After this time, TBAF solution (1 M in THF, 0.12 mL, 0.12 mmol) was added and the resulting mixture was stirred for 5 additional hours at −55 °C. Afterwards, the reaction mixture was neutralized with NH_4Cl aqueous solution. After dilution with brine both phases were separated, and the aqueous phase was extracted with Et_2O. The combined organic extracts were dried over anhydrous $MgSO_4$ and concentrated under vacuum to give a yellowish oily residue which was purified by flash column chromatography on silica gel (hexane/ethyl acetate, 8:2). Finally, a yellow oil was obtained, which was identified as the desired deprotected alkyne 5 (244 mg, 0.96 mmol, 87 % yield). R_f = 0.33 (hexane/ethyl acetate, 8:2); α_D^{25} −54.7 (c 0.8, $CHCl_3$); ^{1}H NMR (400 MHz, $CDCl_3$) δ in ppm: 5.05 (d, J = 8.1 Hz,1H), 4.50 (d, J = 8.1 Hz, 1H), 4.19–4.16 (m, 1H), 4.10 (t ap, J = 8.3 Hz, 1H), 3.91–3.88 (m, 1H), 2.43 (s, 1H), 1.59 (s, 3H), 1.50 (s, 3H), 1.49 (s, 9H); ^{13}C NMR (100.6 MHz, $CDCl_3$) δ in ppm: 154.5, 95.2, 82.1, 81.7, 74.2, 65.2, 64.4, 62.7, 28.5, 26.0, 25.4; HRMS (TOF ES+) for $[M + Na]^+$ $C_{13}H_{21}NNaO_4^+$ (m/z): calculated: 278.1363 found: 278.1367. FT-IR (ATR) ν in cm^{-1}: 3438, 3310, 3256, 2978, 2930, 2116, 1684, 1389, 1365, 1258, 1170, 1067, 1046, 849, 770, 657, 554.

4.1.3. Tert-butyl (S)-4-((S)-(1-dodecyl-1H-1,2,3-triazol-4-yl)(hydroxy)methyl)-2,2-dimethyloxazolidine-3-carboxylate (6)

1-Azidododecane [42] (378 mg, 1.79 mmol) and terminal alkyne **5** (398 mg, 1.56 mmol) were dissolved in dry CH_2Cl_2 (8.5 mL). The solution was stirred at room temperature and a solution of $CuSO_4{\cdot}5H_2O$ (21.3 mg, 0.086 mmol) in distilled H_2O (1.5 mL) followed by a solution of sodium ascorbate (31.6 mg, 0.16 mmol) in distilled H_2O (1.5 mL) were added dropwise. The resulting mixture was stirred at room temperature for 48 h. The reaction mixture was diluted with brine, both phases were separated and the aqueous one was extracted with CH_2Cl_2. The combined organic extracts were dried over anhydrous $MgSO_4$, filtered, and concentrated under reduced pressure. The reaction crude was then purified by flash column chromatography on silica gel (hexane/ethyl acetate, from 3:1 to 3:2), to yield the desired product **6** (715 mg, 1.53 mmol, 98 %) as a colorless oil. R_f = 0.33 (hexane/ethyl acetate, 6:4); α_D^{25} −27.6 (c 0.6, $CHCl_3$); Spectroscopic data of the mixture of both rotamers (a and b): ^{1}H NMR (400 MHz, CD_3OD) δ in ppm: 7.87 (s, 1H), 7.85 (s, 1H), 5.10 (d, J = 3.1 Hz, 1H), 5.04 (d, J = 4.3 Hz, 1H), 4.40–4.35 (m, 4H), 4.26–4.23 (m, 2H), 4.12–4.04 (m, 2H), 3.99–3.89 (m, 2H), 1.92–1.89 (m, 4H), 1.65 (s, 3H), 1.56 (s, 3H), 1.50 (s, 6H), 1.43–1.34 (m, 18H), 1.34–1.26 (m, 36H), 0.90 (t, J = 6.8 Hz, 6H); ^{13}C NMR (100 MHz, CD_3OD) δ for two rotamers in ppm: 154.3 and 153.7, 150.8 and 150.5, 124.0 and 123.8, 95.8 and 95.4, 81.7 and 81.3, 67.6 and 67.5, 65.3 and 65.1, 63.0 and 62.8, 51.3, 33.1, 31.4, 30.77, 30.76, 30.67, 30.60, 30.5, 30.2, 28.6, 27.5, 27.3 and 26.5, 25.0 and 23.8, 23.6, 14.5; HRMS (TOF ES+) for $[M + Na]^+$ $C_{25}H_{46}N_4NaO_4^+$(m/z): calculated: 489.3417 found: 489.3416; FT-IR (ATR) ν in cm^{-1}: 3419, 3135, 2925, 2855, 1698, 1463, 1389, 1173, 1075, 853.

4.1.4. (1S,2S)-2-amino-1-(1-dodecyl-1H-1,2,3-triazol-4-yl)propane-1,3-diol (7)

Protected triazole derivative **6** (720 mg, 1.54 mmol) was dissolved in a H_2O/TFA (1:10, 15.4 mL) mixture and the solution was stirred at room temperature for 1 h 45 min. After this time, the reaction mixture was slowly poured into a saturated aqueous $NaHCO_3$ (350 mL) solution at −10 °C. Bubbling was observed due to neutralization of the excess of TFA. The resulting suspension was extracted with AcOEt. The combined organic extracts were dried over anhydrous $MgSO_4$ and concentrated under vacuum to give a white oily residue. The residue was purified by flash column chromatography on silica gel (CH_2Cl_2/MeOH/Et_3N, 9:1:0.1) to yield the desired aminodiol **12** as a white solid (274 mg, 0.84 mmol, 54 % yield). R_f = 0.12 (CH_2Cl_2/MeOH/Et_3N, 9:1:0.1); α_D^{25} + 1.5 (c 1.0, MeOH); ^{1}H NMR (400 MHz, CD_3OD) δ in ppm: 7.91 (s, 1H), 4.81 (d, J = 6.2 Hz, 1H), 4.40 (t, J = 7.1 Hz, 2H), 3.66 (dd, J = 10.9 Hz, J = 4.3 Hz, 1H), 3.57 (dd, J = 10.9 Hz, J = 6.6 Hz, 1H), 3.19–3.14 (m, 1H), 1.94–1.87 (m, 2H), 1.33–1.29 (m, 18H), 0.90 (t, J = 6.8 Hz, 3H); ^{13}C NMR (100 MHz, CD_3OD) δ in ppm: 150.2, 124.1, 69.1, 63.8, 58.1, 51.4, 33.1, 31.3, 30.77, 30.76, 30.68, 30.60, 30.5, 30.1, 27.5, 23.8, 14.5; HRMS (TOF ES+) for $[M + Na]^+$ $C_{17}H_{34}N_4NaO_2^+$ (m/z): calculated: 349.2579 found: 349.2577; FT-IR (ATR) ν in cm^{-1}: 3333, 3289, 3213, 3150, 2916, 2849, 1617, 1469, 1152, 1065, 827.

4.1.5. N-((1S,2S)-1-(1-dodecyl-1H-1,2,3-triazol-4-yl)-1,3-dihydroxypropan-2-yl)hexanamide (1a)

The reaction was performed as described in general procedure for *N*-acylation, by using hexanoic acid (17.3 μL, 0.14 mmol), EDC (26.5 mg, 0.14 mmol), HOBt (18.9 mg, 0.14) and aminodiol **7** (30.0 mg, 0.092 mmol). Purification of the yellow oily residue thus obtained, by using CH_2Cl_2/MeOH, 96:4 as eluent; furnish ceramide analogue **1a** as a white oil (24.2 mg, 0.056 mmol, 62 % yield). R_f = 0.18 (CH_2Cl_2/MeOH, 96:4); α_D^{25} –33.8 (c 0.4, $CHCl_3$); ^{1}H NMR (400 MHz, $CDCl_3$) δ in ppm: 7.60 (s, 1H), 6.55 (d, J = 6.5 Hz, 1H), 5.65 (bs, 1H), 5.09 (d, J = 2.0 Hz, 1H), 4.90 (bs, 1H), 4.35–4.27 (m, 3H, H-2), 4.17 (dd, J = 12.0 Hz, J = 1.6 Hz, 1H), 3.79 (dd, J = 12.0 Hz, J = 4.8 Hz, 1H), 2.19–2.05 (m, 2H), 1.91–1.84 (m, 2H), 1.55–1.44 (m, 2H), 1.31–1.15 (m, 22H), 0.87 (t, J = 6.5 Hz, 3H), 0.85 (t, J = 7.3 Hz, 3H); ^{13}C NMR (400 MHz, $CDCl_3$) δ in ppm: 175.8, 149.3, 122.7, 71.6, 62.3, 56.4, 50.7, 36.4, 32.0, 31.3, 30.3, 29.73, 29.66, 29.53, 29.46, 29.1, 26.6, 25.5, 22.8, 22.4, 14.3, 14.0; HRMS (TOF ES+) for $[M + Na]^+$ $C_{23}H_{44}N_4NaO_3^+$ (m/z): calculated: 447.3311 found: 447.3309; FT-IR (ATR) ν in cm^{-1}: 3388, 3236, 3064, 2922, 2852, 1734, 1645, 1559, 1211, 1062, 774.

4.1.6. N-((1S,2S)-1-(1-dodecyl-1H-1,2,3-triazol-4-yl)-1,3-dihydroxypropan-2-yl)octanamide (1b)

Compound **1b** was synthesized following the general procedure for *N*-acylation from octanoic acid (21.9 μL, 0.14 mmol), EDC (26.5 mg, 0.14 mmol), HOBt (18.9 mg, 0.14 mmol) and aminodiol **7** (30.0 mg, 0.092 mmol). Purification by using a mixture CH_2Cl_2/MeOH, 96:4 as solvent led ceramide analogue **1b** as a white oil (28.0 mg, 0.062 mmol, 67 % yield). R_f = 0.19 (CH_2Cl_2/MeOH, 96:4); α_D^{25} −4.6 (c 0.41, $CHCl_3$); ^{1}H NMR (400 MHz, $CDCl_3$) δ in ppm: 7.59 (s, 1H), 6.53 (d, J = 6.4 Hz, 1H), 5.63 (bs, 1H), 5.08 (d, J = 1.8 Hz, 1H), 4.35–4.27 (m, 3H), 4.17 (dd, J = 12.1 Hz, J = 1.7 Hz, 1H), 3.79 (dd, J = 12.1 Hz, J = 5.0 Hz, 1H), 2.19–2.05 (m, 2H), 1.92–1.84 (m, 2H), 1.53–1.45 (m, 2H), 1.30–1.22 (m, 26H), 0.87 (t, J = 6.8 Hz, 3H), 0.86 (t, J = 6.9 Hz, 3H); ^{13}C NMR (400 MHz, $CDCl_3$) δ in ppm: 175.9, 149.3, 122.7, 71.8, 62.4, 56.5, 50.8, 36.5, 32.0, 31.8, 30.3, 29.8, 29.74, 29.67, 29.54, 29.47, 29.2, 29.13, 29.08, 26.6, 25.8, 22.8, 22.7, 14.3, 14.2; HRMS (TOF ES+) for $[M + Na]^+$ $C_{25}H_{48}N_4NaO_3^+$ (m/z): calculated: 475.3624 found: 475.3620; FT-IR (ATR) ν in cm^{-1}: 3391, 3234, 3067, 2923, 2852, 1734, 1646, 1558, 1209, 1056, 773.

4.1.7. N-((1S,2S)-1-(1-dodecyl-1H-1,2,3-triazol-4-yl)-1,3-dihydroxypropan-2-yl)decanamide (1c)

Compound **1c** was prepared following the general procedure of *N*-acylation by using decanoic acid (11.9 mg, 0.07 mmol), EDC (13.7 mg, 0.07 mmol), HOBt (9.9 mg, 0.07 mmol) and aminodiol **7** (15.0 mg, 0.046 mmol). After the work-up, the yellow oily residue was purified

(CH_2Cl_2/MeOH, 96:4). Ceramide analogue **1c** was obtained as a white oil (14.1 mg, 0.029 mmol, 63 % yield). $R_f = 0.28$ (CH_2Cl_2/MeOH, 96:4); α_D^{25} −20.8 (*c* 0.75, $CHCl_3$); ^{1}H NMR (400 MHz, $CDCl_3$) δ in ppm: 7.59 (s, 1H), 6.51 (d, *J* = 6.2 Hz, 1H), 5.08 (d, *J* = 1.6 Hz, 1H), 4.37–4.26 (m, 3H, H-2), 4.18 (dd, *J* = 12.1 Hz, *J* = 1.5 Hz, 1H), 3.80 (dd, *J* = 12.1 Hz, *J* = 5.1 Hz, 1H), 2.19–2.05 (m, 2H), 1.92–1.85 (m, 2H), 1.53–1.45 (m, 2H), 1.31–1.17 (m, 30H), 0.87 (t, *J* = 6.7 Hz, 6H); ^{13}C NMR (400 MHz, $CDCl_3$) δ in ppm: 176.0, 149.4, 122.7, 72.1, 62.4, 56.6, 50.8, 36.5, 32.1, 32.0, 30.3, 29.9, 29.8, 29.7, 29.58, 29.55, 29.48, 29.44, 29.43, 29.2, 29.1, 26.6, 25.9, 22.83, 22.82, 14.3; HRMS (TOF ES+) for $[M + H]^+$ $C_{27}H_{52}N_4NaO_3^+$ (*m/z*): calculated: 503.3937 found: 503.3961; FT-IR (ATR) ν in cm^{-1}: 3409, 3236, 3056, 2921, 2850, 1731, 1645, 1569, 1210, 1057, 774.

*4.1.8. Tert-butyl (S)-4-((S)-hydroxy(1-tridecyl-1H-1,2,3-triazol-5-yl) methyl)-2,2-dimethyloxazolidine-3-carboxylate (**8**)*

Cp*RuCl(COD) (46.0 mg, 0.12 mmol) was dissolved in dry and previously degassed toluene (9 mL, toluene was degassed for 1 h with nitrogen purge). A solution of alkyne **5** (442.1 mg, 1.73 mmol) and 1-azidotridecane [42,43] (549 mg, 2.43 mmol) in dry and previously degassed toluene (5.6 mL) was added. The mixture was stirred at room temperature overnight in which time the total consumption of the starting material was observed by TLC analysis. Then, the reaction mixture was filtered through a short path of Celite followed by the evaporation of the solvent under reduced pressure. The residue was purified by flash column chromatography on silica gel (hexane/ethyl acetate, 7:3) and product **8** was obtained in form of a white oil (594 mg, 1.24 mmol, 72 %). $R_f = 0.33$ (hexane/ethyl acetate, 8:2); α_D^{25} −10.4 (*c* 1.0, $CHCl_3$); ^{1}H NMR (400 MHz, $CDCl_3$) δ in ppm: 7.53 (s, 1H), 5.16 (s, 1H), 4.48–4.34 (m, 2H), 4.25 (m, 1H), 4.08–4.04 (m, 1H), 4.00 (dd, *J* = 9.6 Hz, *J* = 6.5 Hz, 1H), 1.99–1.91 (m, 2H), 1.49–1.43 (m, 15H), 1.35–1.24 (m, 20H), 0.87 (t, *J* = 6.7 Hz, 3H); ^{13}C NMR (100.6 MHz, $CDCl_3$) δ in ppm: 153.6, 136.9, 131.6, 94.7, 81.7, 66.4, 64.0, 61.2, 49.4, 32.1, 30.3, 29.83, 29.79, 29.76, 29.7, 29.6, 29.5, 29.2, 28.4, 26.9, 26.8, 24.0, 22.8, 14.3; HRMS (TOF ES+) for $[M + H]^+$ $C_{26}H_{49}N_4O_4^+$ (*m/z*): calculated: 481.3748 found: 481.3751; FT-IR (ATR) ν in cm^{-1}: 3226, 2923, 2852, 1698, 1458, 1364, 1252, 1170, 1099, 1067, 1051, 847, 768, 605, 566, 526.

*4.1.9. (1S,2S)-2-amino-1-(1-tridecyl-1H-1,2,3-triazol-5-yl)propane-1,3-diol (**9**)*

Triazole derivative **8** (570 mg, 1.19 mmol) was dissolved in a H_2O/TFA (1:10, 12.2 mL) mixture and the solution was stirred at room temperature for 1 h 45 min. After this time, the reaction mixture was slowly poured into a saturated aqueous $NaHCO_3$ (250 mL) solution at −10 °C. Bubbling was observed due to TFA neutralization. The resulting suspension was extracted with AcOEt. The combined organic extracts were dried over anhydrous $MgSO_4$ and concentrated under vacuum to give a white oily residue. The residue was purified by flash column chromatography on silica gel (CH_2Cl_2/MeOH/Et_3N, 9:1:0.1) obtaining deprotected product **9** as a white solid (294 mg, 0.86 mmol, 73 % yield).

$R_f = 0.26$ (CH_2Cl_2/MeOH/Et_3N, 9:1:0.1); α_D^{25} −4.0 (*c* 1.1, MeOH); M. p. 105–107 °C; ^{1}H NMR (400 MHz, $CDCl_3$) δ in ppm: 7.72 (s, 1H), 4.80 (d, *J* = 7.3 Hz, 1H), 4.44 (m, 2H), 3.69 (d, *J* = 5.2 Hz, 2H), 3.16 (dt, *J* = 7.3 Hz, *J* = 5.2 Hz, 1H), 1.94 (m, 2H), 1.40–1.26 (m, 20H), 0.90 (t, *J* = 6.7 Hz, 3H); ^{13}C NMR (100.6 MHz, $CDCl_3$) δ in ppm: 139.3, 133.1, 66.0, 62.8, 57.5, 49.8, 33.1, 31.2, 30.79, 30.76, 30.68, 30.6, 30.5, 30.2, 27.7, 23.7, 14.4, 8.46; HRMS (TOF ES+) for $[M + H]^+$ $C_{18}H_{37}N_4O_2^+$ (*m/z*): calculated: 341.2911 found: 341.2920; FT-IR (ATR) ν in cm^1: 3342, 3276, 3121, 2954, 2919, 2848, 1598, 1468, 1375, 1303, 1239, 1123, 1084, 1032, 989, 956, 831, 721, 694, 619.

*4.1.10. N-((1S,2S)-1,3-dihydroxy-1-(1-tridecyl-1H-1,2,3-triazol-5-yl) propan-2-yl)hexanamide (**2a**)*

Following the general procedure, aminodiol **9** (83.5 mg, 0.25 mmol) was *N*-acylated by using hexanoic acid (62 μL, 0.50 mmol), EDC (93.9 mg, 0.49 mmol), and HOBt (66.0 mg, 0.49). The crude was purified employing CH_2Cl_2/MeOH/NH_4OH, 97:3:1 as eluent. Thus, ceramide analogue **2a** was obtained as a white solid (69.2 mg, 0.16 mmol, 64 % yield). $R_f = 0.22$ (CH_2Cl_2/MeOH/NH_4OH, 9:1:0.1); α_D^{25} + 31,7 (*c* 1.1, CH_2Cl_2/MeOH (1:1)); M.p. 56–57 °C; ^{1}H NMR (400 MHz, $CDCl_3$) δ in ppm: 7.51 (s, 1H), 6.78 (d, *J* = 7.7 Hz, 1H), 5.34 (d, *J* = 6.2 Hz, 1H), 5.14–5.12 (m, 1H), 4.44–4.32 (m, 2H), 4.12–4.07 (m, 2H), 4.01 (d, *J* = 11.2 Hz, 1H), 3.69 (d, *J* = 11.2 Hz, 1H), 2.20 (t, *J* = 7.6 Hz, 2H), 1.93–1.86 (m, 2H), 1.59 (quint ap, *J* = 7.5 Hz, 2H), 1.34–1.24 (m, 24H), 0.87 (t, *J* = 6.6 Hz, 6H); ^{13}C NMR (100.6 MHz, $CDCl_3$) δ in ppm: 174.5, 137.8, 132.0, 66.6, 61.4, 53.8, 49.1, 36.7, 32.1, 31.5, 30.4, 29.82, 29.79, 29.7, 29.6, 29.5, 29.3, 26.8, 25.4, 22.8, 22.5, 14.3, 14.1; HRMS (TOF ES+) for $[M + Na]^+$ $C_{24}H_{46}N_4NaO_3^+$ (*m/z*): calculated: 461.3462 found: 461.3465; FT-IR (ATR) ν in cm^{-1}: 3494, 3383, 3275, 3127, 2957, 2917, 2847, 1635, 1550, 1464, 1329, 1251, 1133, 1091, 1065, 1048, 878, 800, 756, 721, 634, 589, 527.

*4.1.11. N-((1S,2S)-1,3-dihydroxy-1-(1-tridecyl-1H-1,2,3-triazol-5-yl) propan-2-yl)octanamide (**2b**)*

The reaction was performed as described in general procedure for *N*-acylation starting from octanoic acid (78 μL, 0.49 mmol), EDC (95.2 mg, 0.50 mmol), HOBt (66.1 mg, 0.49 mmol) and aminodiol **9** (83.4 mg, 0.25 mmol). The resulting yellow oily crude was purified (CH_2Cl_2/MeOH/NH_4OH, 97:3:1), getting ceramide analogue **2b** as a white solid (80.0 mg, 0.17 mmol, 70 % yield). $R_f = 0.23$ (CH_2Cl_2/MeOH/NH_4OH, 9:1:0.1); α_D^{25} + 24.7 (*c* 0.5, CH_2Cl_2/MeOH (1:1)); M.p. 67–68 °C; ^{1}H NMR (400 MHz, $CDCl_3$) δ in ppm: 7.50 (s, 1H), 6.74 (d, *J* = 7.7 Hz, 1H), 5.23–5.22 (m, 1H), 5.14–5.12 (m, 1H), 4.44–4.32 (m, 2H), 4.11–4.06 (m, 1H), 4.02–3.99 (m, 2H), 3.72–3.66 (m, 1H), 2.21 (t, *J* = 7.7 Hz, 2H), 1.94–1.84 (m, 2H), 1.63–1.55 (m, 2H), 1.35–1.24 (m, 28H), 0.87 (t, *J* = 6.6 Hz, 6H); ^{13}C NMR (100.6 MHz, $CDCl_3$) δ in ppm: 174.5, 137.6, 132.0, 66.9, 61.5, 53.8, 49.1, 36.7, 32.1, 31.8, 30.4, 29.83, 29.79, 29.7, 29.6, 29.5, 29.4, 29.3, 29.1, 26.8, 25.8, 22.8, 22.8, 14.3, 14.2; HRMS (TOF ES+) for $[M + H]^+$ $C_{26}H_{51}N_4O_3^+$ (*m/z*): calculated: 467.3956 found: 467.3961; FT-IR (ATR) ν in cm^{-1}: 3459, 3408, 3291, 3126, 3072, 2954, 2918, 2850, 1636, 1544, 1466, 1375, 1325, 1246, 1128, 1065, 1049, 1000, 869, 801, 758, 718, 680, 634, 549.

*4.1.12. N-((1S,2S)-1,3-dihydroxy-1-(1-tridecyl-1H-1,2,3-triazol-5-yl) propan-2-yl)decanamide (**2c**)*

Following the general procedure for *N*-acylation, decanoic acid (84.5 mg, 0.49 mmol), EDC (93.3 mg, 0.49 mmol), HOBt (65.7 mg, 0.49 mmol) and aminodiol **9** (82.5 mg, 0.24 mmol) were reacted. The yellow oily residue was purified using CH_2Cl_2/MeOH/NH_4OH, 97:3:1) tto give ceramide analogue **2c** as a white solid (86.3 mg, 0.17 mmol, 72 % yield). $R_f = 0.27$ (CH_2Cl_2/MeOH/NH_4OH, 9:1:0.1); α_D^{25} −10.3 (*c* 1.1, CH_2Cl_2/MeOH (1:1)); M.p. 79–80 °C; ^{1}H NMR (400 MHz, $CDCl_3$) δ in ppm: 7.57 (s, 1H), 6.54–6.52 (m, 1H), 5.18 (d, *J* = 4.0 Hz, 1H), 4.45–4.34 (m, 2H), 4.040 (bs, 1H), 4.035 (dd, *J* = 15.2 Hz, *J* = 3.5 Hz, 1H), 3.72 (dd, *J* = 15.2 Hz, *J* = 3.5 Hz, 1H), 2.24 (t, *J* = 7.7 Hz, 2H), 1.92 (quint ap, *J* = 7.2 Hz, *J* = 7.2 Hz, 2H), 1.62 (quint ap, *J* = 7.3 Hz, *J* = 7.3 Hz, 2H), 1.33–1.25 (m, 32H), 0.88 (t, *J* = 7.0 Hz, 6H); ^{13}C NMR (100.6 MHz, $CDCl_3$) δ in ppm: 174.8, 138.6, 131.2, 66.1, 61.4, 54.3, 49.8, 36.6, 32.1, 32.0, 30.2, 29.84, 29.80, 29.75, 29.64, 29.61, 29.5, 29.44, 29.41, 29.3, 26.8, 25.8, 22.83, 22.81, 14.3; HRMS (TOF ES+) for $[M + H]^+$ $C_{28}H_{55}N_4O_3^+$ (*m/z*): calculated: 495.4269 found: 495.4274; FT-IR (ATR) ν in cm^{-1}: 3525, 3439, 3284, 3138, 2952, 2915, 2868, 2848, 1743, 1644, 1543, 1469, 1415, 1379, 1327, 1295, 1254, 1232, 1196, 1124, 1115, 1064, 1040, 1027, 865, 762, 718, 696, 614, 580, 526, 496.

4.1.13. 2-dodecylfuran (10) [24]

A solution of furan (0.91 mL, 12.5 mmol) in anhydrous THF (41.7 mL) was cooled down to −78 °C. Then, butyllithium solution (2.5 M in hexanes, 4.7 mL, 11.8 mmol) was added dropwise and the resulting

mixture was stirred at 0 °C for 2 h. After that time, the mixture was cooled down to −40 °C and 1-bromododecane (2 mL, 8.3 mmol) dissolved in dry THF (2.3 mL) was added dropwise. The resulting mixture was stirred at room temperature overnight. Then, a saturated aqueous $NaHCO_3$ solution was added. Both phases were separated, the aqueous phase was diluted with saturated NaCl solution and extracted with AcOEt. The combined organic extracts were washed with saturated NaCl aqueous solution, dried over anhydrous Na_2SO_4 and concentrated under vacuum to give a yellowish oily residue. The residue was purified by flash column chromatography (dichloromethane) on silica gel and a yellow liquid was obtained, which was identified as 2-dodecylfuran, **10**, (1.960 g, 8.34 mmol, 99 %). $R_f = 0.77$ (hexane/ethyl acetate, 8:2); ^{1}H NMR (400 MHz, $CDCl_3$) δ in ppm: 7.29 (dd, $J = 1.85$ Hz, $J = 0.9$ Hz, 1H), 6.27 (dd, $J = 1.85$ Hz, $J = 3.1$ Hz, 1H), 5.97 (m, 1H), 2.61 (t, $J = 7.6$ Hz, 2H), 1.66–1.61 (m, 2H), 1.35–1.26 (m, 18H), 0.88 (t, $J = 7.0$ Hz, 3H); ^{13}C NMR (100 MHz, $CDCl_3$) δ in ppm: 156.8, 140.7, 110.2, 104.6, 32.1, 29.82, 29.79, 29.7, 29.52, 29.51, 29.3, 28.2, 28.1, 22.8, 14.3; HRMS (TOF ES+) for $[M + H]^+$ $C_{16}H_{29}O^+$ (*m/z*): calculated: 237.2213 found: 237.2211; FT-IR (ATR) ν in cm^{-1}: 2953, 2922, 2852, 1597, 1507, 1465, 1146, 1007, 924, 885, 794, 723, 599 cm^{-1}.

4.1.14. Tert-butyl (S)-4-((S)-(5-dodecylfuran-2-yl)(hydroxy)methyl)-2,2-dimethyloxazolidine-3-carboxylate (11)

2-dodecylfuran, **10**, (412 mg, 1.59 mmol) was dissolved in dry THF (8.3 mL). The resulting solution was cooled down to −78 °C and BuLi solution (2.5 M in hexanes, 0.70 mL, 1.75 mmol) was added dropwise. After the addition, the mixture was warmed up to 0 °C and stirred at this temperature for 1 h. Then, dry HMPA (0.38 mL, 2.18 mmol) was added and the mixture was stirred an additional hour at 0 °C. Afterwards, the solution was cooled down to −55 °C and (*S*)-Garner's aldehyde (249 mg, 1.09 mmol) dissolved in dry THF (1 mL) was added. The resulting mixture was stirred at −55 °C overnight. After this time, NH_4Cl saturated aqueous solution was added, both phases were separated and extractions of the aqueous phase with AcOEt were performed. The combined organic extracts were dried over anhydrous Na_2SO_4 and concentrated under vacuum to give a yellowish oily residue. The residue was then dissolved in dry THF/MeOH solution (8 mL, 3:1). $NaBH_4$ (25.2 mg, 0.66 mmol) was added to the solution and the mixture was stirred at room temperature until the total consumption of the residual (*S*)-Garner's aldehyde was observed by TLC analysis. At this point, the mixture was diluted with aqueous NaCl saturated solution and extractions of the aqueous phase with AcOEt were performed. Finally, the combined organic extracts were dried over anhydrous Na_2SO_4 and concentrated under vacuum to give a yellowish oily residue. The residue was purified by flash column chromatography on silica gel (hexane/ethyl acetate, 8:2) and a yellow oil was obtained, which was identified as a diastereomeric mixture of the desired product **11** (420 mg, 0.90 mmol, 83 % yield) in a 7:1 (*anti/syn*) molar relation. $R_f = 0.31$ (hexane/ethyl acetate, 8:2); Data shown for the major isomer (*anti*: ^{1}H NMR (400 MHz, $CDCl_3$) δ in ppm: 6.15 (d, $J = 3.0$ Hz, 1H), 5.91 (d, $J = 3.0$ Hz, 1H), 4.89–4.85 (m, 1H), 4.64 (bs, 1H), 4.35–4.32 (m, 1H), 4.07–4.05 (m, 2H), 2.56 (t, $J = 7.6$ Hz, 2H), 1.66–1.47 (m, 17H), 1.34–1.26 (m, 18H), 0.88 (t, $J = 3.8$ Hz, 3H); ^{13}C NMR δ in ppm: 156.4, 154.3, 151.9, 107.9, 105.3, 94.7, 81.3, 69.9, 64.8, 62.1, 32.1, 29.9, 29.82, 29.79, 29.70, 29.5, 29.4, 28.5, 28.2, 22.8, 14.3; HRMS (TOF ES+) for $[2\,M + Na]^+$ $C_{54}H_{94}N_2NaO_{10}^+$ (*m/z*): calculated: 953.6801 found: 953.6798; FT-IR (ATR) ν in cm^{-1}: 3454, 2924, 2853, 1670, 1457, 1388, 1365, 1255, 1206, 1172, 1093, 1069, 1011, 949, 849, 781, 768, 721, 563, 524, 462.

4.1.15. (1S,2S)-2-amino-1-(5-dodecylfuran-2-yl)propane-1,3-diol (12)

A diastereomeric mixture (7:1, *anti/syn*) of protected furan derivate **11** (422 mg, 0.91 mmol) was dissolved in dry CH_2Cl_2 (9.1 mL). Et_3N (0.89 mL, 6.39 mmol) was added and the resulting mixture was stirred 20 min at room temperature. The mixture was cooled down to 0 °C and TMSOTf (0.50 mL, 2.76 mmol) was added, the reaction mixture was stirred at 0 °C for 3 h. After this time, NH_4Cl saturated solution was added to the reaction mixture. Both phases were separated, the aqueous phase was extracted with CH_2Cl_2 and, afterwards, the combined organic extracts were washed up with $NaHCO_3$ saturated solution, dried over anhydrous $MgSO_4$ and concentrated under vacuum to give a yellow oily residue. Without further purification, the previous crude was dissolved in anhydrous THF (9.1 mL). Then, TBAF solution (1 M in THF, 2.72 mL, 2.72 mmol) was added and the reaction mixture was stirred overnight at room temperature. After this time, a NH_4Cl saturated solution was added to the reaction mixture. Both phases were separated, the aqueous phase was extracted with AcOEt and the combined organic extracts were dried over anhydrous $MgSO_4$ and concentrated under vacuum to give a white oily residue, which was purified by flash column chromatography on silica gel (CH_2Cl_2/MeOH/Et_3N, 95:5:1). A white solid was obtained, identified as a diasteromeric mixture (18:1, *anti/syn*) of the desired aminodiol **12** (286.4 mg, 0.88 mmol, 97 %). $R_f = 0.26$ (CH_2Cl_2/MeOH/NH_4OH, 9:1:0.1); Data shown for the major isomer (1*S*,2*S*): ^{1}H NMR (400 MHz, MeOD) δ in ppm: 6.23 (d, $J = 3.1$ Hz, 1H), 5.99 (d, $J = 3.1$ Hz, 1H), 4.52 (d, $J = 7.1$ Hz, 1H), 3.72 (dd, $J = 11.0$ Hz, $J = 4.1$ Hz, 1H), 3.59 (dd, $J = 11.0$ Hz, $J = 6.5$ Hz, 1H), 3.12–3.08 (m, 1H), 2.61 (t, $J = 7.5$ Hz, 2H), 1.67–1.60 (m, 2H), 1.34–1.27 (m, 18H), 0.90 (t, $J = 6.8$ Hz, 3H); ^{13}C NMR δ in ppm: (100.6 MHz, MeOD) 157.5, 154.3, 109.3, 106.4, 70.1, 64.1, 57.1, 33.1, 30.81, 30.78, 30.73, 30.5, 30.3, 29.2, 28.9, 23.8, 14.47; HRMS (TOF ES+) for $[M + Na]^+$ $C_{19}H_{35}NNaO_3^+$ (*m/z*): calculated: 348.2509 found: 348.2510; FT-IR (ATR) ν in cm^{-1}: 3313, 2955, 2922, 2852, 1653, 1633, 1558, 1541, 1522, 1457, 1260, 1089, 1017, 798.

4.1.16. N-((1S,2S)-1-(5-dodecylfuran-2-yl)-1,3-dihydroxypropan-2-yl) hexanamide (3a)

The reaction was performed as described in general procedure for *N*-acylation starting from hexanoic acid (62 μL, 0.50 mmol), EDC (94.6 mg, 0.49 mmol), HOBt (66.0 mg, 0.49) and aminodiol **12** (79.2 mg, 0.24 mmol) in dry CH_2Cl_2. The resulting yellow oily residue was purified by using CH_2Cl_2/MeOH/NH_4OH, 96:4:1) to afford **3a** as a white solid (79.4 mg, 0.19 mmol, 77 % yield). R_f = 0.11 (CH_2Cl_2/MeOH/NH_4OH, 9.5:0.5:0.1); α_D^{25} −12.0 (*c* 1.1, $CHCl_3$); M.p. 58–59 °C; ^{1}H NMR (400 MHz, $CDCl_3$) δ in ppm: ^{1}H NMR δ in ppm: (400 MHz, $CDCl_3$) *δ* 6.31–6.30 (m, 1H), 6.21 (d, $J = 3.0$ Hz, 1H), 5.92 (d, $J = 3.0$ Hz, 1H), 4.90 (d, $J = 4.4$ Hz, 1H), 4.23 (m, 1H), 3.90 (dd, $J = 11.5$ Hz, $J = 3.4$ Hz, 1H), 3.70 (d, $J = 11.5$ Hz, $J = 3.3$ Hz, 1H), 2.57 (t, $J = 7.7$ Hz, 2H), 2.20 (t, $J = 7.6$ Hz, 2H), 1.64–1.56 (m, 4H), 1.34–1.22 (m, 22H), 0.88 (t, $J = 6.9$ Hz, 3H), 0.87 (t, $J = 6.8$ Hz, 3H);^{13}C NMR (100.6 MHz, $CDCl_3$) δ in ppm: 174.4, 156.8, 151.7, 108.2, 105.5, 69.9, 62.8, 54.5, 36.9, 32.1, 31.5, 29.81, 29.79, 29.78, 29.7, 29.5, 29.4, 28.2, 28.1, 25.5, 22.8, 22.5, 14.3, 14.1; HRMS (TOF ES+) for $[M + Na]^+$ $C_{25}H_{45}NNaO_4^+$ (*m/z*): calculated: 446.3241 found: 446.3234; FT-IR (ATR) ν in cm^{-1}: 3288, 2954, 2923, 2852, 1651, 1636, 1541, 1456, 1418, 1376, 1302, 1259, 1218, 1189, 1057, 1013, 965, 784, 721, 669.

4.1.17. N-((1S,2S)-1-(5-dodecylfuran-2-yl)-1,3-dihydroxypropan-2-yl) octanamide (3b)

Following the general procedure for *N*-acylation, octanoic acid (31 μL, 0.20 mmol), EDC (38.4 mg, 0.20 mmol), HOBt (26.3 mg, 0.20) and aminodiol **12** (31.8 mg, 0.10 mmol) were used in dry CH_2Cl_2. The reaction was quenched and the yellow oily crude using CH_2Cl_2/MeOH/NH_4OH, 96:4:1 to give **3b** as a white solid (26.5 mg, 0.06 mmol, 60 % yield). $R_f = 0.17$ (CH_2Cl_2/MeOH/NH_4OH, 9.5:0.5:0.1); α_D^{25} −15.0 (c 1.0, $CHCl_3$); M.p. 46–47 °C; ^{1}H NMR (400 MHz, $CDCl_3$) δ in ppm: 6.24 (m, 1H), 6.22 (d, $J = 3.3$ Hz, 1H), 5.92 (d, $J = 3.3$ Hz, 1H), 4.91 (t ap., $J = 4.6$ Hz, 1H), 4.26–4.21 (m, 1H), 3.94–4.21 (m, 1H), 3.75–3.70 (m, 1H), 3.39 (bs, 1H), 2.72 (bs, 1H), 2.58 (t, $J = 7.6$ Hz, 2H), 2.22 (t, $J = 7.6$ Hz, 2H), 1.65–1.57 (m, 4H), 1.34–1.22 (m, 26H), 0.88 (t, $J = 6.9$ Hz, 6 H); ^{13}C NMR (100.6 MHz, $CDCl_3$) δ in ppm:174.4, 156.9, 151.7, 108.3, 105.6, 70.1, 63.0, 54.5, 36.9, 32.1, 31.8, 29.82, 29.80, 29.7, 29.5, 29.4, 29.3), 29.2, 28.2, 28.1, 25.9, 22.84, 22.76, 14.3, 14.2; HRMS (TOF ES+)

for $[M + Na]^+$ $C_{27}H_{49}NNaO_4^+$ (*m/z*): calculated: 474.3554 found: 474.3558; FT-IR (ATR) ν in cm^{-1}: 3301, 2955, 2922, 2851, 653, 1636, 1541, 1507, 1458, 1377, 1257, 1086, 1015, 858, 796, 724, 683, 668, 549.

4.1.18. N-((1S,2S)-1-(5-dodecylfuran-2-yl)-1,3-dihydroxypropan-2-yl) decanamide (3c)

The reaction was performed as described in *N*-acylation general procedure by using decanoic acid (84.5 mg, 0.49 mmol), EDC (93.9 mg, 0.49 mmol), HOBt (66.2 mg, 0.49) and aminodiol **12** (75.1 mg, 0.23 mmol) in dry CH_2Cl_2. The resulting yellow oily residue was purified by flash column chromatography on silica gel (CH_2Cl_2/MeOH/NH_4OH, 96:4:1). Ceramide analogue **3c** was thus obtained as a white solid (81.2 mg, 0.17 mmol, 73 % yield). R_f = 0.20 (CH_2Cl_2/MeOH/NH_4OH, 9.5:0.5:0.1); α_D^{25} −14.0 (*c* 1.5, $CHCl_3$); M.p. 38–39 °C; ^{1}H NMR (400 MHz, $CDCl_3$) δ in ppm: 6.26 (d, *J* = 7.7 Hz, 1H), 6.22 (d, *J* = 3.1 Hz, 1H), 5.93 (d, *J* = 3.1 Hz, 1H), 4.91 (d, = 4.4 Hz, 1H), 4.24 (m, 1H), 3.97 (dd, *J* = 11.5 Hz, *J* = 3.8 Hz, 1H), 3.71 (d, *J* = 11.5 Hz, *J* = 3.8 Hz, 1H), 2.57 (t, *J* = 7.7 Hz, 2H), 2.21 (t, *J* = 7.6 Hz, 2H), 1.64–1.56 (m, 4H), 1.33–1.25 (m, 30H), 0.87 (t, *J* = 6.8 Hz, 6H); ^{13}C NMR (100.6 MHz, $CDCl_3$) δ in ppm: 174.4, 156.9, 151.7, 108.3, 105.5, 70.1, 62.9, 54.5, 36.9, 32.1, 32.0, 29.82, 29.80, 29.7, 29.6, 29.5, 29.4, 29.37, 29.36, 28.2, 28.1, 25.9, 22.84, 22.82, 14.27, 14.26; HRMS (TOF ES+) for $[M + Na]^+$ $C_{29}H_{53}NNaO_4^+$ (*m/z*): calculated: 502.3867 found: 474.3866; FT-IR (ATR) ν in cm^{-1}: 3383, 3310, 2918, 2849, 1644, 1620, 1557, 1466, 1378, 1262, 1234, 1102, 1051, 1013, 957, 787, 721, 651, 549, 427.

4.1.19. 2-tridecylcycloprop-2-en-1-one (14)

NaI (2.526 g, 16.85 mmol) and 1-pentadecyne (2 mL, 7.62 mmol) were dissolved in dry THF (10.2 mL) under argon atmosphere in a Schlenck pressure tube. $TMSCF_3$ (5.63 mL, 38.09 mmol) was added to the solution. The Schlenck pressure tube was sealed and the mixture was heated at 110 ℃ while vigorously stirring. After 21 h $NaHCO_3$ saturated aqueous solution was added to the reaction mixture. Both phases were separated, and the aqueous phase was extracted with Et_2O. The combined organic extracts were desiccated with anhydrous $MgSO_4$ and concentrated under vacuum to give a yellowish oily residue. The obtained residue was dissolved in a hexane/AcOH mixture (99:1, 140 mL) and treated with silice at room temperature overnight. Afterwards, the mixture was filtrated under vacuum through a filter plate and extracted with $NaHCO_3$ saturated solution. The organic phase was desiccated with anhydrous $MgSO_4$ and concentrated under vacuum to give a yellowish oily residue. The residue was purified by flash column chromatography on silica gel (gradient: hexane/ethyl acetate, from 7:3 to 6:4) and finally the desired cyclopropenone **14** was obtained as a white solid (1.724 g, 7.29 mmol, 96 % yield). R_f = 0.20 (hexane/ethyl acetate, 1:1); M.p. 41–42 °C; ^{1}H NMR (400 MHz, $CDCl_3$) δ in ppm: 8.40 (s, 1H), 2.64 (t, *J* = 7.3 Hz, 2H), 1.68 (q ap., *J* = 7.4 Hz, 2H), 1.40–1.33 (m, 2H), 1.30–1.17 (m, 20H), 0.84 (t, *J* = 6.6 Hz, 3H); ^{13}C NMR (100.6 MHz, $CDCl_3$) δ in ppm: 170.3, 158.0, 148.2, 32.0, 29.70, 29.68, 29.6, 29.5, 29.4, 29.2, 29.0, 27.5, 25.7, 22.7, 14.2; HRMS (TOF ES+) for $[M + H]^+$ $C_{16}H_{29}O^+$ (*m/z*): calculated: 237.22129 found: 237.22124; FT-IR (ATR) ν in cm^{-1}: 3047, 2957, 2914, 2847, 1877, 1827, 1804, 1745, 1577, 1469, 1460, 1411, 1158, 1032, 886, 874, 715.

4.1.20. 6,6-dimethyl-1-tridecyl-4,8-dioxaspiro[2.5]oct-1-ene (15)

Tridecylcyclopropenone, **14**, (1.005 g, 4.25 mmol) and BF_4OEt_3 (1.215 g, 6.39 mmol) were dissolved in dry CH_2Cl_2 (7 mL) under argon atmosphere. The resulting mixture was vigorously stirred at room temperature for 30 min. Neopentylglycol (888 mg, 8.53 mmol) and Et_3N (1.18 mL, 8.47 mmol) dissolved in dry CH_2Cl_2 (2.3 mL) were added over the previous mixture dropwise. After the addition, the reaction mixture was stirred at room temperature overnight. After this time, $NaHCO_3$ saturated solution was added to the reaction mixture. The organic phase was washed multiple times with $NaHCO_3$ saturated solution, then, desiccated with Na_2SO_4 and concentrated under reduced pressure. A brown oily residue was obtained, which was purified by flash column chromatography on silica gel (hexane/AcOEt, 9:1) to give the desired ketal **15** in form of a yellow liquid (1.218 g, 3.78 mmol, 89 % yield). R_f = 0.40 (hexane/ethyl acetate, 9:1); ^{1}H NMR (400 MHz, $CDCl_3$) δ in ppm: 7.32 (t, *J* = 1.2 Hz, 1H), 3.63 (d, *J* = 10.4 Hz, 2H), 3.59 (d, *J* = 10.4 Hz, 2H), 2.52 (td, *J* = 7.3 Hz, *J* = 1.2 Hz, 2H), 1.62 (q ap, *J* = 7.4 Hz, 2H), 1.40–1.25 (m, 22H), 1.06 (s, 3H), 1.00 (s, 3H), 0.88 (t, *J* = 6.9 Hz, 3H); ^{13}C NMR (100.6 MHz, $CDCl_3$) δ in ppm: 138.2, 115.3, 83.7, 77.3, 32.1, 30.5, 29.83, 29.81, 29.80, 29.76, 29.7, 29.5, 29.4, 29.3, 27.4, 25.1, 22.8, 22.6, 22.3, 14.3; HRMS (TOF ES+) for $[M + H]^+$ $C_{16}H_{29}O^+$ (*m/z*): calculated: 323.29446 found: 323.29373; FT-IR (ATR) ν in cm^{-1}: 2952, 2924, 2852, 1729, 1467, 1393, 1362, 1279, 1217, 1076, 1024, 994, 935, 723.

4.1.21. Tert-butyl (S)-4-((R)-(6,6-dimethyl-2-tridecyl-4,8-dioxaspiro[2.5]oct-1-en-1-yl)(hydroxy)methyl)-2,2-dimethyloxazolidine-3-carboxylate (16)

Protected cyclopropenone **15** (609 mg, 1.89 mmol) and HMPA (0.66 mL, 3.79 mmol) were dissolved in dry THF (8.5 mL) under argon atmosphere. The solution was cooled down to −55 °C and BuLi (0.75 mL, 2.5 M in hexanes, 1.88 mmol) was added dropwise. The mixture was stirred for 30 min at −55 °C and then, (*S*)-Garner's aldehyde (234 mg, 1.05 mmol) dissolved in dry THF (1.9 mL) was added. The resulting mixture was stirred at −55 °C overnight. After this time, an aqueous NH_4Cl saturated solution was added to the reaction mixture, both phases were separated, and the aqueous phase was extracted with dichloromethane. The combined organic extracts were dried over anhydrous Na_2SO_4, filtered and concentrated under vacuum to give a brownish residue, which was purified by flash column chromatography on silica gel (hexane/AcOEt, 8:2). The addition product **16** was obtained as a colourless liquid (438 mg, 76 % yield). R_f = 0.17 Hexane/AcOEt (8:2); α_D^{25} −8,4 (*c* 1.3, $CHCl_3$); ^{1}H NMR (400 MHz, $CDCl_3$, 50 °C) δ in ppm: 5.04–5.03 (m, 1H), 4.16 (br s, 1H), 4.00–3.99 (m, 2H), 3.69–3.64 (m, 2H), 3.56 (d, *J* = 11.0 Hz, 2H), 2.47 (t, *J* = 7.5 Hz, 2H), 1.65–1.57 (m, 6H), 1.50 (s, 9H), 1.37–1.26 (m, 22H), 1.06 (s, 3H), 0.94 (s, 3H), 0.88 (t, *J* = 6.7 Hz, 3H); ^{13}C NMR (100.6 MHz, $CDCl_3$) δ in ppm: 154.0, 130.1, 128.7, 95.0, 84.9, 81.3, 77.7, 77.2, 68.5, 64.8, 61.4, 32.0, 30.4, 29.82, 29.79, 29.78, 29.76, 29.68, 29.55, 29.49, 29.4, 28.5, 27.7, 26.2, 24.5, 22.8, 22.6, 22.2, 14.3; HRMS (ESI+) for $[M + H]^+$ $C_{32}H_{58}NO_6^+$ (*m/z*): calculated: 552.42587, found: 552.42346; FT-IR (ATR) ν in cm^{-1}: 3418, 2953, 2923, 2852, 1811, 1703, 1668, 1466, 1390, 1365, 1259, 1173, 1022, 989, 932, 849, 808, 769, 721, 636, 516.

4.1.22. 2-((1R,2S)-2-amino-1,3-dihydroxypropyl)-3-tridecylcycloprop-2-en-1-one (17)

Compound **16** (438 mg, 0.79 mmol) was dissolved in water (15.3 mL), the solution was cooled down to 0 °C and HCl (4.9 mL, 2 M in Et_2O, 9.8 mmol) was added dropwise. After the addition, the reaction mixture was warmed up to room temperature and stirred for 3 h. After this time, it was concentred under vacuum to obtaining a brown solid residue.

The residue was then dissolved in a CH_2Cl_2/MeOH/NH_4OH (9:1:1) mixture stirred for 30 min and concentrated again under vacuum. The obtained brown solid was the purified by flash column chromatography on silica gel CH_2Cl_2/MeOH/NH_4OH (95:5:1) to furnish the desired aminodiol **17** as a white solid (159 mg, 62 % yield). R_f = 0.20 CH_2Cl_2/MeOH/NH_4OH (9:1:0.1); α_D^{25} + 1.6 (*c* 1.1, MeOH); M.p. = 132–133 °C; ^{1}H NMR δ in ppm (400 MHz, CD_3OD) δ in ppm: 4.75 (dt, *J* = 5.5 Hz, *J* = 1.0 Hz, 1H), 3.66 (dd, *J* = 11.0 Hz, *J* = 5.5 Hz, 1H), 3.61 (dd, *J* = 11.0 Hz, *J* = 5.5 Hz, 1H), 3.09 (q ap, *J* = 5.5 Hz, 1H), 2.74 (td, *J* = 7.2 Hz, *J* = 1.0 Hz, 2H), 1.75 (p, *J* = 5.5 Hz, 2H), 1.46–1.26 (m, 20H), 0.90 (t, *J* = 7.0 Hz, 3H); ^{13}C NMR (100.6 MHz, CD_3OD) δ in ppm: 162.8, 162.0, 161.2, 71.3, 63.6, 57.6, 33.1, 30.9, 30.82, 30.79, 30.76, 30.6, 30.5, 30.4, 30.3, 27.4, 26.8, 23.8, 14.5; HRMS (ESI+) for $[M + H]^+$ $C_{19}H_{36}NO_3^+$ (*m/z*): calculated: 326,26897, found: 326,26923; FT-IR (ATR) ν in cm^{-1}:

3288, 2955, 2920, 2851, 1844, 1615, 1466, 1413, 1377,1048, 889, 720,619, 580, 550.

4.1.23. *N-((1R,2S)-1,3-dihydroxy-1-(3-oxo-2-tridecylcycloprop-1-en-1-yl)propan-2-yl)octanamide (**PR280**)*

Following the general procedure for *N*-acylation**,** octanoic acid (32 μL, 0.20 mmol), EDC (38.8 mg, 0.20 mmol), HOBt (28.1 mg, 0.21 mmol) and aminodiol **17** (66.7 mg, 0.18 mmol) were reacted. After work-up, the yellowish solid residue obtained was purified by using CH_2Cl_2/MeOH/NH_4OH, 95:5:1 as eluent. The resulting solid was recrystallized with pentane and product **PR280** was obtained as a white solid (59.6 mg, 0.13 mmol, 60 % yield). $R_f = 0.09$ CH_2Cl_2/MeOH/NH_4OH (95:5:1); α_D^{25} −41.2 (*c* 0.5, $CHCl_3$); M.p. = 126–127 °C; ^{1}H NMR (400 MHz, $CDCl_3$) δ in ppm: 6.81 (d, $J = 5.2$ Hz, 1H), 5.87 (d, $J = 5.2$ Hz, 1H), 4.82 (d, $J = 5.2$ Hz, 1H), 4.2 (m, 1H), 4.02–3.98 (m, 2H), 3.94–3.89 (m, 1H), 2.67 (t, $J = 7.3$ Hz, 2H), 2.29–2.17 (m, 2H), 1.75–1.68 (m, 2H), 1.59 (p, $J = 7.3$ Hz, 1H), 1.39–1.25 (m, 28H), 0.88 (t, $J = 6.5$ Hz, 6H); ^{13}C NMR (100.6 MHz, $CDCl_3$) δ in ppm: 176.8, 162.1, 160.6, 159.5, 71.8, 61.5, 56.4, 36.4, 32.1, 31.8, 29.8, 29.83, 29.80, 29.77, 29.6, 29.5, 29.4, 29.30, 29.28, 29.1, 26.6, 26.3, 25.8, 22.79, 22.84, 22.76, 14.3, 14.21; HRMS (ESI+) for $[M + H]^+$ $C_{27}H_{50}NO_4^+$ (*m/z*): calculated: 452.37343, found: 452.37360; FT-IR (ATR) ν in cm^{-1}: 3307, 2955, 2920, 2871, 2851, 1838, 1647, 1577, 1546, 1465, 1418, 1377, 1329, 1293, 1264, 1243, 1207, 1122, 1073, 981, 944, 798, 721, 696, 654, 621, 537.

4.2. Biological evaluation

4.2.1. Materials

All reactions sensitive to air and/or moisture. **GT11**, **XM462** and dhCerC6NBD were available in our laboratories. Dulbecco's Modified Eagle Medium, Fetal bovine serum, penicillin and streptomycin, trypsin-EDTA and NADH were from Sigma-Aldrich/Merck.

4.2.2. Cell culture

Human glioblastoma cell lines T98G were cultured at 37 °C in 5 % CO_2 in Dulbecco's Modified Eagle Medium supplemented with 10 % fetal bovine serum and 100 ng/mL each of penicillin and streptomycin.

4.2.3. Desaturase activity in intact cells

To determine the compounds activity on Des1 in intact cells, cells were seeded in 6 well plates at a density of 2.5×10^5 cells/mL. After incubation at 37 °C and 5 % CO_2, the medium was replaced with 1 mL of fresh complete medium containing the inhibitory candidates, positive control (**XM462** or **GT11**) or negative control (EtOH or DMSO) with a 10 μM final concentration. After incubation at 37 °C for 20 h, 1 mL of fresh complete medium containing dhCerC6NBD (fluorescent marked substrate) with a 10 μM concentration was added to the medium and incubated for an additional 4 h. The media was then collected in an Eppendrof tube, cells were washed with PBS (400 μL/well) and the washing solution was combined with the collected media. After collecting the media, cells were detached by trypsinization (400 μL/well Trypsin-EDTA, 5 min. incubation at 37 °C, 5 % CO_2), 600 μL of medium was then added to the cell suspension and the solution was transferred to an Eppendorf tube. One millilitre of MeOH was added to each Eppendorf tube (medium and cell suspension) which was then vortexed and kept at 4 °C overnight. After centrifugation (10,000 rpm for 3 min), the supernatants were transferred to HPLC vials and either 25 μL (media) or 100 μL (cells) were injected in to HPLC. Analyses were performed with an Alliance apparatus coupled to a fluorescence detector using a C18 reversed-phase column eluted with 15 % H_2O and 8 % acetonitrile, both with a 0.1 % trifluoroacetic acid, flowing at 1 mL/min. The detector was set at an excitation wavelength of 470 nm and the emission wavelength at 530 nm. Each sample was run for up to 15 min.

4.2.4. Desaturase activity in cell lysates

The needed volume (1×10^6 cells/sample) of a cell suspension in medium was transferred to a falcon tube and centrifugated at 400 g at 4 °C during 3 min, supernatant was discarded, and the obtained pellet was washed twice with PBS. Cellular lysates were obtained by suspending the previously obtained pellet with 0.25 M sacarose solution, applying a probe sonication (Branson Sonifier 150, 50 % amplitude, microtip 2.4 mm) and centrifuging. 100 μL of the supernatant (1×10^6 cells) were transferred to an Eppendorf tube with 85 μL dhCerNBD solution (in PBS, final concentration: 10 μM), 85 μL inhibitor candidate solution (in DMSO or EtOH, final concentration: 10 μM), 35 μL NADH solution (in PBS, final concentration: 2.25 mM). The mixture was incubated for 4 h at 37 °C. After this time, one millilitre of MeOH was added to the Eppendorf tube, which was then vortexed and kept at 4 °C overnight. After centrifugation (10,000 rpm for 3 min), the supernatant was transferred to HPLC vials and 25 μL were injected in to HPLC. Analyses were performed with an Alliance apparatus coupled to a fluorescence detector using a C18 reversed-phase column eluted with 15 % H_2O and 8 % acetonitrile, both with a 0.1 % trifluoroacetic acid, flowing at 1 mL/min. The detector was set at an excitation wavelength of 470 nm and the emission wavelength at 530 nm. Each sample was run for up to 15 min.

4.2.5. IC_{50} determination

Cellular lysates were obtained by suspending the pellet with 0.25 M sacarose solution, applying a probe sonication (Branson Sonifier 150, 50 % amplitude, microtip 2.4 mm) and centrifuging. 100 μL of the supernatant (1×10^6 cells) were transferred to an Eppendorf tube with 85 μL dhCerNBD solution (in PBS, final concentration: 10 μM), 85 μL inhibitor candidate solution (in DMSO or EtOH, final concentrations between 0.1 and –10 μM), 30 μL NADH solution (in PBS, final concentration: 2.25 mM). The mixture was incubated for 4 h at 37 °C. After this time, 700 μL of MeOH was added to the Eppendorf tube, which was then vortexed and kept at 4 °C overnight. After centrifugation (10,000 rpm for 3 min), the supernatant was transferred to HPLC vials and 25 μL were injected in to HPLC. Analyses were performed with an Alliance apparatus coupled to a fluorescence detector using a C18 reversed-phase column eluted with 15 % H_2O and 8 % acetonitrile, both with a 0.1 % trifluoroacetic acid, flowing at 1 mL/min. The detector was set at an excitation wavelength of 470 nm and the emission wavelength at 530 nm. Each sample was run for up to 15 min.

4.3. Docking study

GT11, **XM462**, the natural substrate (**dhCer**), and the synthesized compounds **1b**, **2b**, **3c**, and **PR280** were drawn in MOE and underwent ligand preparation using openbabel 3 version 3.0.0 [44] for format conversion, ChemAxon's cxcalc software [45] for tautomer and stereoisomer generation and Corina version 4.3.0 software [46] to generate 3D conformers. After the preparation steps, the rDock software [47] was used for cavity generation and all molecules were docked in the generated binding pocket.

GT11, **XM462** and **dhCer** were subjected to exhaustive docking (50 independent genetic algorithm optimizations) using a free docking protocol. Each ligand's top 10 docking poses were visualised, from which the best scoring pose forming hydrogen bonds through the polar head was selected as the candidate-binding pose. This was necessary to compensate for the insufficient desolvation penalty of rDock's native scoring function. Compounds **1b**, **2b**, **3c**, and **PR280** were docked using a modified protocol that included pharmacophoric restraints to achieve the same effect. The restraints consisted of flat bottom potentials (2 Å radius) for two hydrogen bond donors located near the Fe_2O_2 prosthetic group.

CRediT authorship contribution statement

Pablo Rivero: Investigation, Methodology. **Varbina Ivanova:** Formal analysis, Investigation, Methodology. **Xavier Barril:** Investigation, Methodology. **Mireia Casampere:** Investigation, Methodology. **Josefina Casas:** Investigation, Methodology. **Gemma Fabriàs:** Formal analysis, Investigation, Methodology. **Yolanda Díaz:** Investigation, Methodology, Supervision, Writing – original draft, Writing – review & editing. **M. Isabel Matheu:** Investigation, Methodology, Supervision, Writing – original draft, Writing – review & editing.

Declaration of competing interest

The authors declare that they have no known competing financial interests or personal relationships that could have appeared to influence the work reported in this paper.

Acknowledgements

We thank Grant PID2021-125923OB-I00 funded by Ministerio de Ciencia e Innovación, Spain (MCIN) and Agencia Estatal de Investigación, Spain (AEI), MCIN/AEI/10.13039/501100011033, and by "European Regional Development Fund (ERDF), A way of making Europe". P.R. acknowledges Universitat Rovira i Virgili, Spain, for a predoctoral fellowship (2019PMF-PIPF-36), as well as Generalitat de Catalunya (Secretaria d'Universitats i Recerca), Spain, and European Social Found (ESF), for a predoctoral FI fellowship (FI2021/B00241).

Appendix A. Supplementary data

Supplementary data to this article can be found online at https://doi.org/10.1016/j.bioorg.2024.107233.

References

[1] C. Michel, G. Van Echten-Deckert, J. Rother, K. Sandhoff, E. Wang, A.H. Merrill, Characterization of ceramide synthesis. A dihydroceramide desaturase introduces the 4,5-trans-double bond of sphingosine at the level of dihydroceramide, J. Biol. Chem. 272 (1997) 22432–22437.

[2] a) G. Fabriàs, J. Muñoz-Olaya, F. Cingolani, P. Signorelli, J. Casas, V. Gagliostro, R. Ghidoni, Dihydroceramide desaturase and dihydrosphingolipids: debutant players in the sphingolipid arena, Prog. Lipid Res. 51 (2012) 82–94;
b) C.K. Savile, G. Fabriàs, P.H. Buist, Dihydroceramide delta(4) desaturase initiates substrate oxidation at C-4, J. Am. Chem. Soc. 123 (2001) 4382–4385.

[3] a) F. Lachkar, P. Ferré, F. Foufelle, A. Papaioannou, Dihydroceramides: their emerging physiological roles and functions in cancer and metabolic diseases, Am. J. Physiol. Endocrinol. Metab. 320 (2021) E122–E130;
b) M.M. Siddique, Y. Li, B. Chaurasia, V.A. Kaddai, S.A. Summers, Dihydroceramides: From Bit Players to Lead Actors, J. Biol. Chem. 290 (2015) 15371–15379.

[4] a) W. Zheng, J. Kollmeyer, H. Symolon, A. Momin, E. Munter, E. Wang, S. Kelly, J. C. Allegood, Y. Liu, Q. Peng, H. Ramaraju, M.C. Sullards, M. Cabot, A.H. Merrill, Ceramides and other bioactive sphingolipid backbones in health and disease: Lipidomic analysis, metabolism and roles in membrane structure, dynamics, signaling and autophagy, Biochim. Biophys. Acta - Biomembr. 1758 (2006) 1864–1884;
b) S. Hernández-Tiedra, G. Fabriàs, D. Dávila, Í.J. Salanueva, J. Casas, L. R. Montes, Z. Antón, E. García-Taboada, M. Salazar-Roa, M. Lorente, J. Nylandsted, J. Armstrong, I. López-Valero, C.S. McKee, A. Serrano-Puebla, R. García-López, J. González-Martínez, J.L. Abad, K. Hanada, P. Boya, F. Goñi, M. Guzmán, P. Lovat, M. Jäättelä, A. Alonso, G. Velasco, Dihydroceramide accumulation mediates cytotoxic autophagy of cancer cells via autolysosome destabilization, Autophagy 12 (2016) 2213–2229.

[5] G. Triola, G. Fabriàs, A. Llebaria, Synthesis of a Cyclopropene Analogue of Ceramide, a Potent Inhibitor of Dihydroceramide Desaturase, Angew. Chem. Int. Ed. 40 (2001) 1960–1962.

[6] G. Triola, G. Fabriàs, M. Dragusin, L. Niederhausen, R. Broere, A. Llebaria, G. Van Echten-Deckert, Specificity of the Dihydroceramide Desaturase Inhibitor *N*-[(1*R*,2*S*)-2- Hydroxy-1- hydroxymethyl -2- (2-tridecyl -1- cyclopropenyl) ethyl] octanamide (GT11) in Primary Cultured Cerebellar Neurons, Mol. Pharmacol. 66 (2004) 1671–1678.

[7] G. Triola, G. Fabriàs, J. Casas, A. Llebaria, Synthesis of cyclopropene analogues of ceramide and their effect on dihydroceramide desaturase, J. Org. Chem. 68 (2003) 9924–9932.

[8] J.M. Munoz-Olaya, X. Matabosch, C. Bedia, M. Egido-Gabás, J. Casas, A. Llebaria, A. Delgado, G. Fabriàs, Synthesis and biological activity of a novel inhibitor of dihydroceramide desaturase, ChemMedChem. 3 (2008) 946–953.

[9] a) P.H. Buist, H.G. Dallmann, R.R. Rymerson, P.M. Seigel, P. Skala, Use of sulfur as an oxidant detector, Tetrahedron Lett. 29 (1988) 435–438;
b) K.E. Hovik, O.S. Spydevold, J. Bremer, Thia fatty acids as substrates and inhibitors of stearoyl-CoA desaturase, Biochim. Biophys. Acta, Lipids Lipid Metab. 1349 (1997) 251–256.

[10] C. Bedia, G. Triola, J. Casas, A. Llebaria, G. Fabriàs, Analogs of the dihydroceramide desaturase inhibitor GT11 modified at the amide function: synthesis and biological activities, Org. Biomol. Chem. 3 (2005) 3707–3712.

[11] L. Camacho, F. Simbari, M. Garrido, J.L. Abad, J. Casas, A. Delgado, G. Fabriàs, 3-Deoxy-3,4-dehydro analogs of XM462. Preparation and activity on sphingolipid metabolism and cell fate, Bioorg. Med. Chem. 20(2012) 3173-3179.

[12] M. Casasampere, Y.F. Ordoñez, A. Pou, J. Casas, Inhibitors of dihydroceramide desaturase 1: Therapeutic agents and pharmacological tools to decipher the role of dihydroceramides in cell biology, Chem. Phys. Lipids 197 (2016) 33–44.

[13] a) J. Guasch, I. Giménez-Nueno, I. Funes-Ardoiz, M. Bernús, M.I. Matheu, F. Maseras, S. Castillón, Y. Díaz, Enantioselective Synthesis of Aminodiols by Sequential Rhodium-Catalysed Oxyamination/Kinetic Resolution: Expanding the Substrate Scope of Amidine-Based Catalysis, Chem. Eur. J. 24 (2018) 4635–4642;
b) J. Llaveria, A. Beltrán, W.M.C. Sameera, A. Locati, M.M. Díaz-Requejo, M. I. Matheu, S. Castillón, F. Maseras, P.J. Pérez, Chemo-, Regio-, and Stereoselective Silver-Catalyzed Aziridination of Dienes: Scope, Mechanistic Studies, and Ring-Opening Reactions, J. Am. Chem. Soc. 136 (2014) 5342–5350;
c) J. Guasch, Y. Díaz, M.I. Matheu, S. Castillón, Rhodium-catalyzed regio- and stereoselective oxyamination of dienes via tandem aziridination/ring-opening of dienyl carbamates Chem, Commun. 55 (2014) 7344–7347;
d) J.A. Morales-Serna, J. Llaveria, Y. Díaz, M.I. Matheu, S. Castillón, Recent Advances in the Synthesis of Sphingosine and Phytosphingosine, Molecules of Biological Significance, Curr. Org. Chem. 14 (2010) 2483–2521;
e) J. Llaveria, A. Beltrán, M.M. Díaz-Requejo, M.I. Matheu, S. Castillón, P.J. Pérez, Efficient Silver-Catalyzed Regio- and Stereospecific Aziridination of Dienes, Angew. Chem. Int. Ed. 49 (2010) 7092–7095;
f) J.A. Morales-Serna, Y. Díaz, M.I. Matheu, S. Castillón, Synthesis of D/L-erythro-Sphingosine Using a Tethered Aminohydroxylation Reaction as the Key Step, Synthesis 5 (2009) 710–712;
g) J. Llaveria, Y. Díaz, M.I. Matheu, S. Castillón, An Efficient and General Enantioselective Synthesis of Sphingosine, Phythosphingosine, and 4-Substituted Derivatives, Org. Lett. 11 (2009) 205–208;
h) J.A. Morales-Serna, J. Llaveria, Y. Díaz, M.I. Matheu, S. Castillón, Asymmetric sulfur ylide based enantioselective synthesis of D-erythro-sphingosine, Org. Biomol. Chem. 6 (2008) 4502–4504;
i) M. Escudero-Casao, A. Cardona, R. Beltrán-Debón, Y. Díaz, M.I. Matheu, S. Castillón, Fluorinated triazole-containing sphingosine analogues. Syntheses and in vitro evaluation as SPHK inhibitors, Org. Biomol. Chem. 16 (2018) 7230–7235;
j) M. Corro-Morón, A. Granell, V. Ivanova, E. Domingo, R. Beltrán-Debón, X. Barril, M.-J. Sanz, M.I. Matheu, S. Castillón, Y. Díaz, Revealing 2-dimethylhydrazino-2-alkyl alkynyl sphingosine derivatives as sphingosine kinase 2 inhibitors: Some hints on the structural basis for selective inhibition, Biorg. Chem. 121 (2022) 105668–105684.

[14] a) 1,2,3-Triazole moieties have the capability of binding with enzymes and receptors via weak interactions such as π-π stacking interactions, hydrogen bonds, iron chelation, CH-π interactions. They can suffer *N*-oxidation in some cases: A. Massarotti, S. Aprile, V. Mercalli, E. Del Grosso, G. Grosa, G. Sorba, G.C. Tron, Are ,4- and ,5-disubstituted 1,2,3-triazoles good pharmacophoric groups?, ChemMedChem 9 (2014) 2497-2508; b) They behave as olefinomimetic elements: E. Bonandi, M.S. Christodoulou, G. Fumagalli, D. Perdicchia, G. Rastelli, D. Passarella, The 1,2,3-triazole ring as a bioisostere in medicinal chemistry, Drug Discov.Today 22 (2017) 572-58; c) Furans are also able to display most of the interactions present in triazoles as π-π stacking interactions: R. G. Huber, M.A. Margreiter, J.E. Fuchs, S. von Grafenstein, C.S. Tautermann, K. R. Liedl, T. Fox, Heteroaromatic π-Stacking Energy Landscapes, J. Chem. Inf. Model. 54 (2014) 37-379; d) The presence of the oxygen atom was expected to be beneficial towards a possible chelation: Y. Zhan, X. Ying Wang, H. Shao, Adv. Chem. Res. 5 (2012) 33; e) The furan ring could undergo ring oxidation: L.A. Peterson, Reactive metabolites in the biotransformation of molecules containing a furan ring, Chem. Res. Toxicol. 26 (2013) 6-25.

[15] A. Pou, J.-L. Abad, Y.F. Ordóñez, M. Garrido, J. Casas, G. Fabriàs, A. Delgado, From the Configurational Preference of Dihydroceramide Desaturase-1 towards Δ6-Unsaturated Substrates to the Discovery of a New Inhibitor, Chem. Commun. 53 (2017) 4394–4397.

[16] P. Herold, Synthesis of D-*erythro*- and D-*threo*-Sphingosine Derivatives from L-Serine, Helv. Chim. Acta. 71 (1988) 354–362.

[17] F.F. Wong, S.H. Chuang, S. Yang, Y.-H. Lin, W.-C. Tseng, S.-K. Lin, J.-J. Huang, One-pot ethynylation and catalytic desilylation in synthesis of mestranol and levonorgestrel, Tetrahedron 66 (2010) 4068–4072.

[18] a) R. Huisgen, 1,3-Dipolar Cycloadditions. Past and Future, Angew. Chem. Int. Ed. 10 (1963) 565–632;
b) R. Huisgen, Kinetics and Mechanism of 1,3-Dipolar Cycloadditions, Angew. Chem. Int. Ed. 11 (1963) 633–696.

[19] The geometry of 1,4-regioisomer is closer to *E* than Z double bond, with a distance for the substituents of the heterocycle equivalent to one carbon longer (5.04 Å *vs* 3.92Å). See: D. G. Ghiano, A. de la Iglesia, N. Liu, P. J. Tonge, H. R. Morbidoni, G. R. Labadie, Antitubercular activity of 1,2,3-triazolyl fatty acid derivatives, Eur. J. Med. Chem. 125 (2017) 842-852. For this reason, alkyne **5** was reacted with 1-

azidododecane, having one less carbon than the alkylic chain connected to the double bond in the natural ceramide.

[20] W.G. Kim, M.E. Kang, J.B. Lee, M.H. Jeon, S. Lee, J. Lee, B. Choi, P.M.S.D. Cal, S. Kang, J.-M. Kee, G.J.L. Bernardes, J.-U. Rohde, W. Choe, S.Y. Hong, Nickel-Catalyzed Azide-Alkyne Cycloaddition To Access 1,5-Disubstituted 1,2,3-Triazoles in Air and Water, J. Am. Chem. Soc. 139 (2017) 12121–12124.

[21] a) Review about RhAAC, J.R. Johansson, T. Somfai, A.S. Stalsmeden, N. Kann, Ruthenium-Catalyzed Azide Alkyne Cycloaddition Reaction: Scope, Mechanism, and Applications, Chem. Rev. 116 (2016) 14726–14768;
b) L. Zhang, X.G. Chen, P. Xue, H.H.Y. Sun, I.D. Williams, K.B. Sharpless, V. V. Fokin, G.C. Jia, Ruthenium-catalyzed cycloaddition of alkynes and organic azides, J. Am. Chem. Soc. 127 (2005) 15998–15999;
c) RhAAC in propargylic alcohols, M.M. Majireck, S.M. Weinreb, A study of the scope and regioselectivity of the ruthenium-catalyzed [3 + 2]-cycloaddition of azides with internal alkynes, J. Org. Chem. 71 (2006) 8680–8683.

[22] B.C. Boren, S. Narayan, L.K. Rasmussen, L. Zhang, H.T. Zhao, Z.Y. Lin, G.C. Jia, V. V. Fokin, Ruthenium-catalyzed azide-alkyne cycloaddition: scope and mechanism, J. Am. Chem. Soc. 130 (2008) 8923–8930.

[23] Both regioisomers can be clearly differentiated by ^{13}C NMR spectroscopy based on the different chemical shift of triazole CH: X. Creary, A. Anderson, C. Brophy, F. Crowell, Z. Funk. Method for assigning structure of 1,2,3-triazoles, J. Org. Chem. 77 (2012) 8756−8761.

[24] L. Eschen-Lippold, T. Draeger, A. Teichert, L. Wessjohann, B. Westermann, S. Rosahl, N. Arnold, Antioomycete Activity of γ-Oxocrotonate Fatty Acids against P. infestans, J. Agric. Food Chem. 57 (2009) 9607–9612.

[25] These conditions were successfully used in the synthesis of vinylated analogues of sphingosine 1-phosphate: G. Pons, D. Riba, M. Casasampere, E. Izquierdo, J.-L. Abad, G. Fabriàs, P. G. Rodríguez-Ortega, J.J. López-González, M. Montejo, J. Casas, A. Delgado, A Mechanism-Based Sphingosine-1-phosphate Lyase Inhibitor, J. Org. Chem. 85 (2020) 419−429.

[26] O. Nieto-Faza, C. Silva-López, R. Álvarez, A. Lera, Theoretical Study of the Electrocyclic Ring Closure of Hydroxypentadienyl Cations, Chem. Eur. J. 10 (2004) 4324–4333.

[27] J. Quintana, M. Barrot, G. Fabriàs, F. Camps, A model study on the mechanism of inhibition of fatty acyl desaturases by cyclopropene fatty acids, Tetrahedron 54 (1998) 10187–10198.

[28] M. Cohen, U. Bretler, A. Albeck, Peptidyl cyclopropenones: Reversible inhibitors, irreversible inhibitors, or substrates of cysteine proteases? Protein Sci. 22 (2013) 788–799.

[29] F. Wang, T. Luo, J. Hu, Y. Wang, H.S. Krishnan, P.V. Jog, S.K. Ganesh, G.K. S. Prakash, G.A. Olah, Synthesis of gem-difluorinated cyclopropanes and cyclopropenes: trifluoromethyltrimethylsilane as a difluorocarbene source, Angew. Chem. Int. Ed. 50 (2011) 7153–7157.

[30] Z.L. Cheng, Q.Y. Chen, Difluorocarbene Chemistry: A simple Transformation of 3,3-*gem*-Difluoropropenes to Cyclopropenones, Chin. J. Chem. 24 (2006) 1219–1224.

[31] M. Passiniemi, A.M.P. Koskinen, Garner's aldehyde as a versatile intermediate in the synthesis of enantiopure natural products, Beilstein J. Org. Chem. 9 (2013) 2641–2659.

[32] a) J. Jumper, R. Evans, A. Pritzel, T. Green, M. Figurnov, O. Ronneberger, K. Tunyasuvunakool, R. Bates, A. Zidek, A. Potapenko, A. Bridgland, C. Meyer, S. A. A. Kohl, A. J. Ballard, A. Cowie, B. Romera-Paredes, S. Nikolov, R. Jain, J. Adler, T. Back, S. Petersen, D. Reiman, E. Clancy, M. Zielinski, M. Steinegger, M. Pacholska, T. Berghammer, D. Silver, O. Vinyals, A. W. Senior, K. Kavukcuoglu, P. Kohli, D. Hassabis, Applying and improving AlphaFold at CASP14, Proteins 89 (2021) 1711-1721; b) "AlphaFold Protein Structure Basadate" can be found under https://alphafold.ebi.ac.uk/**2021** (accessed: 22 September 2021); c) "AlphaFold open source code" can be found under https://github.com/deepmind/alphafold **2021** (accessed: 22 September 2021); AlphaFold2 source code and model parameters publications: d) J. Jumper, R. Evans, A. Pritzel, T. Green, M. Figurnov, O. Ronneberger, K. Tunyasuvunakool, R. Bates, A. Zidek, A. Potapenko, A. Bridgland, C. Meyer, S. A. A. Kohl, A. J. Ballard, A. Cowie, B. Romera-Paredes, S. Nikolov, R. Jain, J. Adler, T. Back, S. Petersen, D. Reiman, E. Clancy, M. Zielinski, M. Steinegger, M. Pacholska, T. Berghammer, S. Bodenstein, D. Silver, O. Vinyals, A. W. Senior, K. Kavukcuoglu, P. Kohli, D. Hassabis, Highly accurate protein structure prediction with AlphaFold, Nature, 596 (2021), 583-589; e) K. Tunyasuvunakool, J. Adler, Z. Wu, T. Green, M. Zielinski, A. Žídek, A. Bridgland, A. Cowie, C. Meyer, A. Laydon, S. Velankar, G. J. Kleywegt, A. Bateman, R. Evans, A. Pritzel, M. Figurnov, O. Ronneberger, R. Bates, S.A.A. Kohl, A. Potapenko, A.J. Ballard, B. Romera-Paredes, S. Nikolov, R. Jain, E. Clancy, D. Reiman, S. Petersen, A.W. Senior, K. Kavukcuoglu, E. Birney, P. Kohli, J. Jumper, D. Hassabis, Highly accurate protein structure prediction for the human proteome, Nature 595 (2021) 590-596; Potential of AlphaFold 2 in drug discovery: f) A. Mullard, What does AlphaFold mean for drug discovery?, Nature Rev. Drug Discov. 20 (2021) 725-727.

[33] M. Akdel, D.E.V. Pires, E. Porta Pardo, J. Jänes, A.O. Zalevsky, B. Mészáros, P. Bryant, L.L. Good, R.A. Laskowski, G. Pozzati, A. Shenoy, W. Zhu, P. Kundrotas, V. Ruiz Serra, C.H.M. Rodrigues, A.S. Dunham, D. Burke, N. Borkakoti, S. Velankar, A. Frost, J. Basquin, K. Lindorff-Larsen, A. Bateman, A.V. Kajava, A. Valencia, S. Ovchinnikov, J. Durairaj, D.B. Ascher, J.M. Thornton, N.E. Davey, A. Stein, A. Elofsson, T.I. Croll, P. Beltrao, A structural biology community assessment of AlphaFold2 applications, Nat. Struct. Mol. Biol. 29 (2022) 1056–1067.

[34] The models lack any ligands (metals, cofactors, small molecules, DNA, and other proteins): a) A. David, S. Islam, E. Tankhilevich, M.J.E. Sternberg, The AlphaFold Database of Protein Structures: A Biologist's Guide, J. Mol. Biol. 434 (2022) 167336-167341; b) T.J. Lane, Protein structure prediction has reached the single-structure frontier, Nat. Methods 20 (2023) 170-173.

[35] Molecular Operating Environment (MOE), Chemical Computing Group ULC, 1010 Sherbooke St, West, Suite #910, Montreal, QC, Canada, 2019.01;.

[36] Only three cysteine residues (Cys 79, Cys100 and Cys 154) can be observed outside the active site of the enzyme, two of them in a pheripheral area of Des1 (Cys100 and Cys 154).

[37] This fact could also suggest that the mechanism for stearoyl-CoA desaturase inhibition by sterculic acid (a cyclopropene fatty acid) might not take place via the reaction of the cyclopropene moiety with cysteine residues located in the binding site either. See: R. Peláez, A. Pariente, Á. Pérez-Sala, I. M. Larráyoz, Sterculic Acid: The Mechanisms of Action beyond Stearoyl-CoA Desaturase Inhibition and Therapeutic Opportunities in Human Diseases, Cells 9 (2020) 140-160.

[38] In the docking, it was taken into account that the active compounds are analogs of the natural substrate, which implies that the binding mode would be similar that one of the natural substrate. Following this approach and knowing that the C4-C5 bond dehydrogenation is catalyzed by the diiron-dioxo complex, it has been considered docking poses with the cyclopropene ring of **GT11** close to the complex.

[39] For dimethylsulfide-methanol complex, the binding energy of O-H…S is lower than the H-bond energy for the corresponding oxygen analog. F. Wennmohs, V. Staemmler, M.J. Schindler, Theoretical investigation of weak hydrogen bonds to sulfur, Chem. Phys. 119 (2003) 3208-3218.

[40] Committing molecular dynamic simulations with Des1 is not obvious. On one side, the parametrization of the prosthetic group is complicated. On the other hand, the appearance of the lower part of the protein is completely hydrophobic, which indicates that it is inserted into the membrane. For that reason, the protein would have to be placed into the membrane to have an accurate result.

[41] Some efficient sphingosine kinase inhibitors, such as SKI II and ABC294640, inhibit Des1 as an off-target effect. These non-ceramide-type compounds showed an 80% (at 10 μM) and 40% (at 30 μM) of Des1 inhibition in cell lysates respectively. SKI II: F. Cingolani, M. Casasampere, P. Sanllehí, J. Casas, J. Bujons, G. Fabriàs, Inhibition of dihydroceramide desaturase activity by the sphingosine kinase inhibitor SKI II, J. Lipid Res. 55 (2014) 1711-1720. ABC294640: H. Venant, M. Rahmaniyan, E.E. Jones, P. Lu, M. B. Lilly, E. Garret-Mayer, R.R. Drake, J.M. Kraveka, C.D. Smith, C. Voelkel-Johnson, The Sphingosine Kinase 2 Inhibitor ABC294640 Reduces the Growth of Prostate Cancer Cells and Results in Accumulation of Dihydroceramides *In Vitro* and *In Vivo*, Mol. Cancer Ther. 14 (2015), 2744-2752.

[42] a) Synthesis: J. Hu, T. Zhu, C. He, Y. Zhang, Q. Zhang, G. Zou, Chiral induction, transfer and modulation in C_3-symmetric columnar liquid crystalline assemblies, *J. Mater. Chem. C*, 207, **5**, 535-542; b) Characterization: P.L. Huestis, N. Lease, C. E. Freye, D.L. Huber, G.W. Brown, D.L. McDonald, T. Nelson, C.J. Snyder, V. W. Manner, Radiolytic degradation of dodecane substituted with common energetic functional groups, RSC Adv 3 (2023) 9304–935.

[43] Characterization: C. Liu, X. Wang, Z. Li, L. Cui, C. Li, Silver-Catalyzed Decarboxylative Radical Azidation of Aliphatic Carboxylic Acids in Aqueous Solution, J. Am. Chem. Soc. 37 (205) 9820-9823.

[44] N.M. O'Boyle, M. Banck, C.A. James, C. Morley, T. Vandermeersch, G. R. Hutchison, Open Babel: An open chemical toolbox, J. Cheminform 33 (2011) 1–14.

[45] ChemAxon software was used for drawing, displaying and characterizing chemical structures, ChemAxon (https://www.chemaxon.com).

[46] Chemoinformatics ProgramPackage CORINA Classic, developed and distributed by Molecular Networks GmbH, Nuremberg, Germany and Altamira LLC, Columbus, OH, USA. www.mn-am.com.

[47] S. Ruiz-Carmona, D. Alvarez-Garcia, N. Foloppe, A.B. Garmendia-Doval, S. Juhos, P. Schmidtke, X. Barril, R.E. Hubbard, S.D. Morley, rDock: A Fast, Versatile and Open Source Program for Docking Ligands to Proteins and Nucleic Acids, PLoS Computational Biology 10 (2014) e1003571–e1003577.